UNIVERSITI TEKNOLOGI MARA

METABOLIC PATHWAY OF *CIS*-UCA UPON ULTRAVIOLET B (UVB) EXPOSURE USING ^{1}H NUCLEAR MAGNETIC RESONANCE (NMR) SPECTROSCOPY, MOLECULAR DOCKING AND CELL VIABILITY OF HUMAN KERATINOCYTES (HACAT) CELL LINES

AINA YUSRINA BINTI ALI MUSA

MSc

February 2026

UNIVERSITI TEKNOLOGI MARA

METABOLIC PATHWAY OF *CIS*-UCA UPON ULTRAVIOLET B (UVB) EXPOSURE USING ^{1}H NUCLEAR MAGNETIC RESONANCE (NMR) SPECTROSCOPY, MOLECULAR DOCKING AND CELL VIABILITY OF HUMAN KERATINOCYTES (HACAT) CELL LINES

AINA YUSRINA BINTI ALI MUSA

Thesis submitted in fulfilment
of the requirements for the degree of
Master of Science
(Pharmacology)

Faculty of Pharmacy

February 2026

CONFIRMATION BY PANEL OF EXAMINERS

I certify that a Panel of Examiners has met on 4 November 2025 to conduct the final examination of Aina Yusrina binti Ali Musa on her Master of Science Thesis entitled "Metabolic Pathway of Uraconic Acid (UCA) upon Ultraviolet B (UVB) Exposure using ^{J}H Nuclear Magnetic Resonance (NMR) Spectroscopy, Molecular Docking and Cell Viability of Human Keratinocytes (HaCaT) Cell Lines" in accordance with Universiti Teknologi MARA Act 1976 (Akta 173). The Panel of Examiners recommends that the student be awarded the relevant degree. The Panel of Examiners was as follows:

Mahmathi Karuppannan, PhD
Associate Professor
Faculty of Pharmacy
Universiti Teknologi MARA
(Chairman)

Zolkapli Eshak, PhD
Senior Lecturer
Faculty of Pharmacy
Universiti Teknologi MARA
(Internal Examiner)

Wan Iryani Wan Ismail, PhD
Professor
Faculty of Science & Marine Enviroment
Universiti Malaysia Terengganu
(External Examiner)

PROFESSOR DR HJH ZURAEDA IBRAHIM
Dean
Institute of Postgraduates Studies
Universiti Teknologi MARA

Date: 27 February 2026

AUTHOR'S DECLARATION

I declare that the work in this, thesis was carried out in accordance with the regulations of Universiti Teknologi MARA. It is original and is the result of my own work, unless otherwise indicated or acknowledged as referenced work. This thesis has not been submitted to any other academic institution or non-academic institution for any degree or qualification.

I hereby acknowledge that I have been supplied with the Academic Rules and Regulations for Postgraduate, Universiti Teknologi MARA, regulating the conduct of my study and research.

Name of Student	Aina Yusrina binti Ali Musa
Student ID. No.	2023292796
Programme	Master of Science (Pharmacology) - PH776
Faculty	Pharmacy
Thesis Title	Metabolic Pathway of Uraconic Acid (UCA) upon Ultraviolet B (UVB) Exposure using ^{J}H Nuclear Magnetic Resonance (NMR) Spectroscopy, Molecular Docking and Cell Viability of Human Keratinocytes (HaCaT) Cell Lines
Signature of Student	
Date	27 February 2026

ABSTRACT

Urocanic acid (UCA), a histidine metabolite, is found in the stratum corneum protects and modulates the immune system. Metabolism of photoisomerization *trans-XJCA* to *cis-UCA* is unknown. In 2001, Kinuta *et al.* (2001) proposed *cis-UCA* metabolism pathway but did not clarify the conversion of glutathione conjugates, GS(CIE) to cysteine conjugates, Cys (CIE), leaving a critical mechanistic gap. The primary goal of this study was to investigate the *cis-UCA* metabolic pathway via conjugation with sulphide-derivative chemicals to resolve this unknown phase. Briefly, Nuclear Magnetic Resonance (NMR) metabolomic approach was used to study the reaction of *cis-UCA* with various sulphide donors including N-acetylcysteine (NAC), glutathione (GSH), L-cysteine, sodium hydrosulphide (NaHS) and sodium disulphide (Na2S2) in a cell-free system. Next, a molecular docking analysis was performed to evaluate the interaction of glutathione-S-transferase (GST) with glutathione conjugate, followed by bioassay analysis using Human Keratinocyte Cells (HaCaT). From the results, it was found that *cis-UCA* can readily react with the reactive sulphur species (RSS) donors with no involvement of GST enzyme. A new compound named 4-imidazoleacrylic acid-3-thiol was discovered when the *cis-UCA* reacted with NaHS. Furthermore, although the original pathway reported that the formation of these GS(CIE) and Cys (CIE) is catalysed by GST, results show that both compounds can form even without GST, indicating that the reaction can occur non-enzymatically. Next, through molecular docking experiments, the GS(CIE) shows a greater binding affinity with GST than the reference drug sulforaphane, implying a potential regulatory role of GS(CIE) towards the physiological function of GST. The *in vitro* studies showed that UVB exposure together with *cis-UCA* significantly reduced cell viability, although the presence of sulphide donors appeared to alleviate toxicity. This study gives new insight into the *cis-UCA* metabolism and perhaps sheds light on the potential role of UCA in general as a photo transmitter compound. Overall, this study illustrates that *cis-UCA* engages in non-enzymatic conjugation with RSS, resulting in the formation of novel metabolites, 4-imidazoleacrylic acid-3-thiol. Significantly, RSS co-treatment inhibited *cis-UCA*-enhanced UVB cytotoxicity, confirming a protective role of sulphide donors. These results modify the old GST-dependent model and endorse an alternate RSS-driven pathway in *cis-UCA* metabolism, with effects for UCA's role in UVB-induced skin reactions.

ACKNOWLEDGEMENT

First and foremost, I would like to express my deepest gratitude to Allah SWT for granting me the strength, patience, and perseverance to complete this research project.

I would like to extend my heartfelt appreciation to my supervisor, Dr. Noreen, for her invaluable guidance, constructive feedback, and unwavering support throughout the course of my study. Her expertise and encouragement have been instrumental in shaping this research from its conception to its completion.

I would also like to extend my thanks to Dr. Hisyam, who, despite not being my official supervisor, has offered tremendous help, advice, and encouragement throughout this journey. His willingness to share knowledge and provide guidance has been a great source of motivation, significantly contributing to the progress of my work.

Special thanks also go to Dr. Zafirah for her generous assistance, expertise, and advice in molecular docking experiments. Her guidance in this aspect of my research has been invaluable and greatly enhanced the quality of my results. Her insightful comments and helpful suggestions have also improved the quality of this thesis.

I am sincerely grateful to Dr Noor Hidayah, Professor Dr. Mizaton, the laboratory staff and fellow postgraduate students in the faculty lab for their assistance, friendship, and the many discussions that enriched my research experience. Special thanks to those who provided technical support during my molecular docking experiments, *in vitro* assays, and data analysis.

Finally, I dedicate this achievement to my beloved family, whose endless love, prayers, and sacrifices have been my source of strength and motivation. To my friends, thank you for standing by me through the challenges and celebrating every small victory along the way.

TABLE OF CONTENTS

LIST OF TABLES

LIST OF FIGURES

LIST OF SYMBOLS

mbols

*	$p < 0.05$ versus control group (statistically significant)
**	$p < 0.01$ versus control group (highly significant)
n	$p < 0.05$ versus *cis-UCA I cis-UCA* + UVB group (statistically significant)
##	$p < 0.01$ versus *cis-UCA I cis-UCA* + UVB group (highly significant)
,	Plus-minus; used to indicate standard error of the mean (SEM) or standard deviation (SD)
a	Greek letter alpha; used in biochemical nomenclature (e.g., TNF-a)
P	Greek letter beta; used in biochemical nomenclature (e.g., IL-ip)

LIST OF ABBREVIATIONS

Abbreviations

ID NOESY	One-dimensional Nuclear Overhauser Effect Spectroscopy
5-HT2A	5-Hydroxytryptamine Receptor 2A
8-OHdG	8-Hydroxy-2'-deoxyguanosine
ACQ	Acquisition
AD	Atopic Dermatitis
AmDock	Automated Molecular Docking
ANOVA	Analysis of Variance
ASK1	Apoptosis Signal-Regulating Kinase 1
BBO	Bruker BioSpin Operator
cis-UCA	cw-Urocanic Acid
CO2	Carbon Dioxide
Cys(CIE)	Cysteine-cz's-Urocanic Acid Adduct
CysSSH	Cysteine Persulfide
DMEM	Dulbecco' s Modified Eagle Medium
DMSO	Dimethyl Sulfoxide
DNA	Deoxyribonucleic Acid
ECM	Extracellular Matrix
EGFR	Epidermal Growth Factor Receptor
ERK	Extracellular Signal-Regulated Kinase

FBS	Fetal Bovine Serum
FID	Free Induction Decay
GSH	Reduced Glutathione
GS(CIE)	Glutathione-cz's-Urocanic Acid Adduct
GSSH	Glutathione Persulfide
GSSG	Oxidised Glutathione
GST	Glutathione S-Transferase
TT_{rT}	Human Adult Low-Calcium High-Temperature Keratinocyte Cell Line
HMBC	Heteronuclear Multiple Bond Correlation
HOD	Hydrogen Deuterium Oxide
HSQC	Heteronuclear Single Quantum Coherence
H_2S	Hydrogen Sulfide
IFN-y	Interferon Gamma
IgE	Immunoglobulin E
IL-ip	Interleukin-1 Beta
IL-6	Interleukin-6
IL-10	Interleukin-10
ImAc	Imidazole Acetate
ImCOOH	Imidazole Carboxylic Acid
JNK	c-Jun N-Terminal Kinase
MAPK	Mitogen-Activated Protein Kinase

MATLAB	Matrix Laboratory
MDA	Malondialdehyde
MMPs	Matrix Metalloproteinases
MMP-1	Matrix Metalloproteinase-1
MMP-3	Matrix Metalloproteinase-3
MMP-9	Matrix Metalloproteinase-9
MTT	3-(4,5-Dimethylthiazol-2-yl)-2,5-Diphenyltetrazolium Bromide
NAC	N-Acetylcysteine
NaHS	Sodium Hydrosulfide
Na_2S_2	Sodium Disulfide
NF-KB	Nuclear Factor Kappa-Light-Chain-Enhancer of Activated B Cells
NMR	Nuclear Magnetic Resonance
NOESYPR	Nuclear Overhauser Effect Spectroscopy Presaturation
OPLS-DA	Orthogonal Partial Least Squares Discriminant Analysis
PBS	Phosphate-Buffered Saline
PCA	Principal Component Analysis
PDB	Protein Data Bank
PyMOL	Python Molecular Graphics System
RD	Relaxation Delay
ROS	Reactive Oxygen Species
RSS	Reactive Sulfur Species
SD	Standard Deviation

SEM	Standard Error of the Mean
SIMCA-P	Soft Independent Modeling of Class Analogy-P
SPSS	Statistical Package for the Social Sciences
TNF-a	Tumour Necrosis Factor Alpha
TSP	Trimethylsilyl Propionate
trans-UCA	*trans-Uvocamc* Acid
UCA	Urocanic Acid
UV	Ultraviolet
UVA	Ultraviolet A
UVB	Ultraviolet B
UVC	Ultraviolet C
VIP	Variable Importance in Projection

LIST OF NOMENCLATURE

Nomenclatures

$C_6H_6N_2O_2$	Chemical formula for Urocanic Acid
L-cysteine	Sulphur-containing amino acid
mM	Millimolar concentration (10^{3} mol/L)
uM	Micromolar concentration (10^{6} mol/L)
nm	Nanometre (wavelength unit)
^{D}C	Degrees Celsius
	Hour(s)
nM/cm^2	Nanomoles per square centimetres (UV dose
Type I collagen	Collagen protein type I in skin.
Type III collagen	Collagen protein type III in skin
Ultraviolet (UV)	Electromagnetic radiation from 100-400 nm
5-HT2A	Serotonin receptor subtype
MHz	Megahertz (frequency unit)
mg	Milligram (mass unit)
mL	Millilitre (volume unit)
ppm	Parts per million (concentration unit)
mm	Minute (time unit)
uL	Microliter (volume unit)

CHAPTER 1
INTRODUCTION

1.1 Research Background

Urocanic acid (UCA) is a byproduct of histidine catabolism in the skin, liver, and brain (Tuna, Sporkel, Barbatti, & Thiel, 2018). It serves as a primary epidermal chromophore localised within the stratum corneum and exists as its *trans* isomer. UCA can undergo UV-induced photoisomerisation from the *trans-UCA* to the *cis-UCA* form in a dose-dependent manner, ultimately reaching a photo-stationary state, which consists of approximately 60% of *cis-UCA* (Hart & Norval, 2021a; McLoone *et al.*, 2005). The half-life for this compound is approximately 12 days, as it can be excreted in the urine. This compound can persist on the skin for approximately 3 weeks after exposure and acts as a natural sunscreen to protect the skin (Kammeyer *etal*, 1997).

Urocanase is an enzyme responsible for breaking down *trans-urocanic* acid *(trans-UCA)* into other metabolites that can be utilized in other pathways, such as the glutamate synthesis pathway (Yu *etal*, 2022). This enzyme is found exclusively in the liver and brain, and its absence in human skin led to *cis-UCA* accumulation. This accumulation has been associated with immunosuppressive activity and alteration in cellular antioxidant balance. Previous research suggests that *cis-UCA* may increase reactive oxygen species (ROS) levels and reduce the activity of glutathione-dependent antioxidant enzymes, including catalase and glutathione reductase, in keratinocytes (Kaneko *et al.*, 2011). Under Ultraviolet B (UVB) irradiation, characterized by heightened glutathione depletion and oxidative stress (Panich et al., 2016), the buildup of *cis-UCA* may further compromise the antioxidant defense system, consequently affecting inflammatory and stress-response signalling.

It was initially believed that UCA could act as a natural sunscreen, as it can absorb UV radiation, thereby protecting against cutaneous disease. However, it was subsequently discovered that the *cis* isomer could induce immunosuppression of the skin, leading to other diseases, such as skin cancer, atopic dermatitis, and urticaria (Hart & Norval, 2021b; Pham *et al.*, 2017). Additionally, *cis-UCA* induced apoptotic cell

death in human keratinocyte cells by generating intracellular reactive oxygen species (ROS) through the epidermal growth factor receptor (EGFR) signaling pathway (Kaneko *etah*, 2011). The formation of ROS plays a vital role in oxidative stress, which can lead to cellular damage and inflammation. In this context, reactive sulfur species (RSS), such as hydrogen sulfide (H2S) and other poly sulfides, can interact with ROS and have been shown to play a crucial role in regulating oxidative stress and modulating cellular redox status (Munteanu *et ah,* 2023), making them a vital component in understanding skin reactions to UV radiation.

Reactive sulphur species (RSS) are well known to be endogenously produced in abundance in many species (Iciek *et ah,* 2022), and they exist in various poly sulfide forms with distinct redox-active or reactive chemical properties (Lau *et ah,* 2019). Given the crucial regulatory and protective function of RSS, it is evident that any disturbance in their balance can result in certain pathological diseases. Impaired sulphur or redox signalling leads to atopic dermatitis, wherein oxidative stress and altered thiol metabolism contribute to epidermal barrier failure (Bertino *etah,* 2020). Altered sulfur species and glutathione imbalance are associated with psoriasis, a disorder characterized by increased generation of ROS and dysregulated keratinocyte redox signaling (Dobrica *et ah,* 2019). These examples highlight the importance of maintaining balanced RSS levels to support normal cutaneous physiology. Hydrogen sulfide (H2S), an example of RSS, serves a pivotal role in the skin, including vasodilation, wound healing, and the management of conditions such as psoriasis and melanoma. H2S exerts its antioxidant effect on the skin by reducing intracellular ROS production, improving skin conditions in diabetes mellitus wound healing (Denizalti, 2024).

The role of *cis-XJCA* as a regulatory element for skin health needs more elucidation. Therefore, this study aims to investigate the metabolism of *cis-XJCA. A* study was conducted to investigate the capacity of organic and inorganic sulphide donors, including N-acetylcysteine (NAC), glutathione (GSH), L-cysteine, sodium hydrosulphide (NaHS), and sodium disulphide (Na2S2), particularly the persulphide compounds, to react with *cis-XJCA* in the presence of UVB irradiation. This aims to enhance understanding of the role of *cis-XJCA* in maintaining skin health. The

conjugation of *cis-UCA* with GSH, mediated by GST, has been proposed as the primary elimination pathway of UCA from the body via sweat or urine (Kinuta *et al*, 2001). In contrast to the GSH conjugation pathway, super sulphides can directly form conjugates with electrophiles without the need for catalytic actions (Zhang *et al.*, 2024), such as those mediated by GST.

Due to the limited information on cz's-UCA-sulfide derivative conjugation, further exploration of the UCA metabolism pathway is imperative, particularly in the skin. There is a potential presence of various *cis-UCA* and sulfur derivatives in an interactome, detectable through nuclear magnetic resonance (NMR) spectroscopy. This experiment was further extended to perform a molecular docking analysis between GS(CIE) and GST to explore the potential binding interactions concerning GST binding affinity and its mechanism. In addition, the viability of HaCaT cells was observed after being treated with *cis-UCA* and a sulphide donor. The cz's-UCA-sulfide derivative interactome is expected to provide promising new insights into the underlying mechanisms of skin-related conditions.

1.2 Problem Statement

UCA is a naturally occurring chemical on the skin with photoprotective properties (Ali Musa *etal.,* 2025). UV radiation's isomerisation of *trans-UCA* to the *cis* isomer is the key step in initiating skin pathogenesis (Wei, 2019). *Cis-UCA* is then excreted through urine and sweat in a polar form of cz's-UCA-sulfide derivative conjugate (Kinuta *et al.,* 2003). However, skin-related diseases and hypersensitivity appear to be inversely correlated with the amount of *cis-UCA* in the skin after exposure to UV radiation. *Cis-UCA* has been associated with immunosuppressive effects in the skin, including impairing Langerhans cell function via Tumour Necrosis Factor-alpha (TNF-a) pathways and promoting oxidative stress through ROS generation (Gibbs & Norval, 2011). However, contradictory evidence suggests it may also exert context-dependent protective functions. This contradictory data highlights the need for more mechanistic research, especially to ascertain whether interactions with reactive sulfur species or UVB-induced redox modifications influence the dual biological behavior of *cis-UCA.* While *cis-UCA* has been linked to UV-induced immune suppression and potential DNA damage in cutaneous models (Mathews *etal,* 2011), studies in non-skin

tissues, such as retinal pigment epithelial cells, have shown anti-inflammatory activity and protection against UVB-induced inflammasome activation and genotoxicity (Lu *et ah*, 2021). This contradiction raises questions about the different effects of *cis-UCA*, specifically how conjugation with RSS may affect its biological activity and alter its function in skin health, shifting from harmful to protective.

A preliminary analysis was conducted to understand the intertwined relationship between the *cis-UCA* and UV irradiation in relation to the *in vitro* skin model, the HaCaT cell line. In this experiment, treatment with *cis-UCA* alone, without exposure to UV, can reduce the viability of the *in vitro* model. This result suggests that the accumulation of *cis-UCA* may potentially degrade the physiological function of healthy skin. Indeed, exposure of the subjects to UV irradiation alone resulted in a significant reduction in the number of healthy cells. However, exposure of the cells to UV irradiation and *cis-UCA* exhibited better cellular survivability. Interestingly, the combination of a sulphide donor, *cis-UCA*, and UV irradiation further improves the survival of the cells. Based on these experiments, the potential interaction between UV irradiation, UCA, and endogenous RSS requires further examination.

In addition, despite the pathway that was proposed by Kinuta *et ah* (2001), the underlying mechanism by which the GS(CIE) is converted into the Cys(CIE) remains to be elucidated. It requires empirical evidence, as they did not explain or prove the proposed process between GS(CIE) and Cys (CIE) formation. Despite the unresolved nature of the *cis-UCA* metabolism pathway, researchers have heavily relied upon the incomplete pathway since 2001, underscoring the need for further clarification. This demonstrates that this pathway holds paramount importance for ensuring the integrity and accuracy of scientific inquiry in this field. Hence, it is essential to revisit and conduct a thorough investigation of the pathway study to enhance our understanding of *cis-UCA* metabolism.

Moreover, Kinuta's proposed pathway demonstrates biochemical constraint as the GS(CIE) to Cys (CIE) demands substantial energy to remove two amino acids: glutamate and glycine. This mechanistic difficulty process poses practical challenges and concerns about the pathway's biological plausibility and metabolic feasibility.

Unravelling this can bridge a significant information gap regarding the *cis-UCA* metabolism pathway. This study has the potential to uncover novel insights into its underlying mechanisms and, most importantly, to untangle the probable misunderstood *cis-UCA* metabolism pathway, which will pave the way for future investigations in this field.

1.3 Research Objectives

The increasing prevalence of skin-related disorders due to UV irradiation has significant implications for global public health and healthcare systems. Despite the extensive research in this field, a notable gap exists in our understanding of *cis-UCAs* physiological role and pathological responses, particularly its function in counteracting UV radiation. Generally, this study aimed to bridge the gap by conducting a mechanistic analysis of the metabolism of this *cis-UCA* compound, focusing on the cellular response to UVB irradiation in human keratinocyte (HaCaT) cell lines. Specific objectives were:

a) To characterise the interaction of *cis-UCA* and various sulphide donors in a cell-free system using Nuclear Magnetic Resonance (NMR)
b) To analyse the potential binding interactions between glutathione conjugate GS(CIE) and glutathione-s-transferase (GST) through a molecular docking study.
c) To measure the cytoprotective effect of cis-UCA-RSS conjugates in the human keratinocyte (HaCaT) cell line irradiated with UVB using a cell viability assay.

1.4 Research Question

i) How is the interaction between *cis-UCA* and various sulphide donors in a cell-free system observed?
ii) How does the glutathione conjugate GS(CIE) possibly interact with glutathione-s-transferase (GST) at molecular level?
iii) What is the possible impact of *cis-UCA* and sulphide donor treatments on cell survivability in human keratinocytes (HaCaT) cell lines exposed to UVB irradiation?

1.5 Significance of the Study

This study attempts to deepen the understanding of the *cis-UCA* metabolism pathway and explore its potential role in skin health. Results from this study might be helpful as potential preventative and therapeutic measures for UV-induced skin-related illnesses, especially photoaging and atopic dermatitis. Acquiring knowledge of this pathway may contribute to the development of skin health remedies that protect against damage caused by UV radiation, especially in areas with a high UV index. In the long run, having this knowledge could encourage people to take proactive measures to safeguard their skin and mitigate the risk of developing UV-related skin diseases.

Other than that, findings from the proposed study will establish new perspectives on the vital role of cz's-UCA-sulphide donor-UV interactome as a determining factor between healthy and pathological skin. Understanding the biochemistry behind the skin's photoprotective processes will significantly impact the development and effectiveness of skin care products. The frequency of UV-related skin conditions, including atopic dermatitis and photoaging, continues to grow despite technological advancements. Therefore, a deeper understanding of skin biochemistry could pave the way for creating more effective and tailored skincare solutions, addressing the growing demand for protection against UV-induced skin damage.

Furthermore, this study aims to understand the skin metabolite *cis-UCA*, which is well-known for its role in UV protection, as it provides crucial information on how *cis-UCA* can be leveraged to enhance skin health and prevent UV-induced skin disorders. This study may help identify biomarkers for skin diseases, with a focus on atopic dermatitis. It could pave the way for developing new detection kits for early diagnosis and intervention. Early detection is crucial for effectively managing symptoms, reducing inflammation, alleviating discomfort, and improving the quality of life for individuals affected by these conditions. Healthcare professionals can implement timely interventions to control and manage the severity of the disease progression by pinpointing specific biomarkers indicative of these diseases at an early age. This research contributes to the scholarly understanding of a crucial biological compound and represents a significant step toward the global pursuit of sustainable health, particularly in the realm of dermatological well-being.

CHAPTER 2
LITERATURE REVIEW

2.1 Introduction

UCA is a natural metabolite in the epidermis that exists in a *trans* state and contributes to the skin barrier function. This compound is crucial for shielding the body from infections, external threats, and UV light. Generally, it helps with pH regulation, immunological modulation, and UV absorption (Hart & Norval, 2021a). The enzyme histidase converts L-histidine into *trans-UCA,* the main isomer in the stratum corneum (Norval, 2001). Upon UV exposure, *trans-XJCA* undergoes photoisomerisation into *cis-*UCA, altering its biological activity (McLoone *etah,* 2005). In addition to its function as a UV-absorbing molecule, *cis-UCA* has been linked to several UV-related skin diseases, including inflammatory skin disorders, skin cancer, and photoaging (Peltonen *etal.,* 2014).

Although *cis-UCA* has long been classified as an immunosuppressive agent (Gibbs & Norval, 2011), new research suggests that it may also have a dual function in disease pathogenesis and skin protection, highlighting the ambivalent nature of this molecule. According to new research, it plays a role in immunological signaling pathways that lead to skin aging and disease progression, including those involving oxidative stress, inflammatory cytokines, and matrix metalloproteinases (MMPs) (Verma *et ah,* 2024). This literature explains the photobiology, metabolic pathways, and pathological implications of *cis-UCA,* focusing on its conflicting functions in skin health and disease.

The molecular composition of *cis-UCA* and the differences in chemical structure between *trans-UCA* will be discussed first to provide a groundwork for a thorough understanding of its function in skin physiology. Chemical structures shown in Figure 2.1, where *cis-UCA* with molecular formula $C_6H_6N_2O_2$, also known as imidazole-4-acrylic acid, is a histidine derivative characterised by an imidazole ring and a propenoic acid side chain. The difference between trans and cis forms is that, in the *cis* form, the double bond between the second and third carbon atoms is in the *"cis"*

configuration, meaning that the hydrogen atoms attached to the carbons on the double bond are on the same side, creating a bent shape (Norval, 2001).

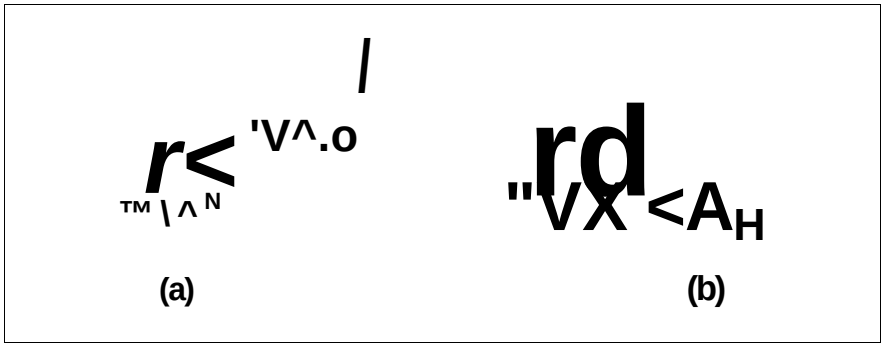

Figure 2.1 Chemical Structures (a) *Trans-UCA* and (b) Cz's-UCA was Generated usingRCSB.org

UCA is found at uniquely high levels in the stratum corneum, the outermost layer of human skin, with relatively constant concentrations in various body sites. In 2017, a study by Pham *et al.* found that the UCA level in patients with chronic spontaneous urticaria (CSU) and atopic dermatitis was higher than in the normal control group. This suggests that the accumulation of *cis-XJCA* on the skin is associated with the development of certain skin diseases in patients. UCA is a product of the amino acid histidine, formed by the enzyme histidase as a *trans-isomer.* This compound can be photoisomerized from *trans-UCA* form into *cis-UCA* form in a dose-independent manner (McLoone *et al,* 2005). UCA is an endogenous molecule of skin, an essential component of hygroscopic and pH-regulating materials, and a photoprotective agent in our skin (Peltonen *etal,* 2014). This compound is a significant absorber of UV light in the skin and acts as a natural sunscreen (Verma *etal,* 2024).

2.2 Skin Structure

The skin is the largest human organ, acting as the primary defense against the environment (Denisow-Pietrzyk *et al,* 2021). It not only acts as a barrier but also hosts molecules that maintain structural and biochemical integrity (Baker *et al,* 2023). Its functions include temperature regulation and protection against ultraviolet (UV) light, trauma, pathogens, microorganisms, and toxins (Prohic, 2024; Mirzayev, 2025). The

skin also plays a crucial role in immunologic surveillance, sensory perception, the control of insensible fluid loss, and overall homeostasis (Lopez-Ojeda *etal.*, 2022).

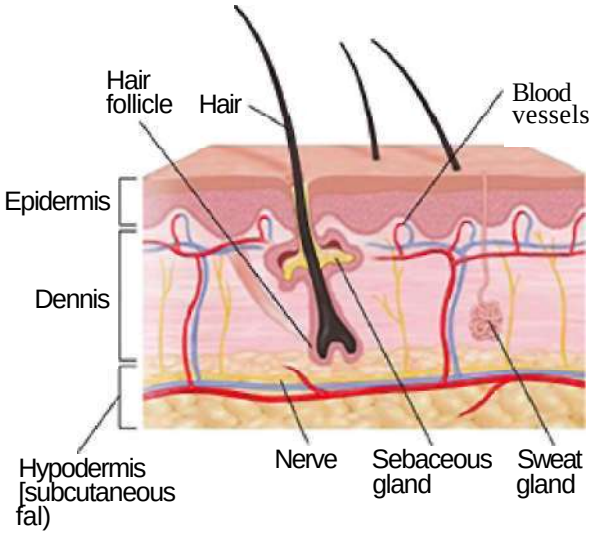

Figure 2.2 Schematic Representation of Human Skin Anatomy Showing the Epidermis, Dermis, and Hypodermis by Johns Hopkins Medicine (n.d.)

Human skin is highly adaptive, with varying thicknesses and specialized functions at different body sites (Peate, 2021). As shown in Figure 2.2, of skin anatomy, it consists of three layers: the epidermis, dermis, and hypodermis (Milner, 2023). One of the key components that helps to build and strengthen the skin is histidine (Holecek, 2020; Solano, 2020). The metabolism of histidine occurs in the stratum corneum, where histidine will break down into histamine and urocanic acid. Histidine and its metabolite, specifically, urocanic acid (UCA), can be found in high concentrations in the stratum corneum, the outermost layer of human skin (Musa *etal.*, 2025). Given that the stratum corneum has a high amount of UCA and absorbs the majority of incoming UV radiation, this layer becomes the predominant site where UV-induced photoisomerization occurs. Understanding UV-skin interactions is therefore critical for interpreting UV-induced skin responses.

2.3 Ultraviolet Radiation (UV) and Skin Photobiology

Ultraviolet (UV) radiation is a crucial environmental factor influencing skin biology. In the environmental context, UV is the most significant controllable risk factor for skin cancer and many other environmentally influenced skin disorders (D'Orazio *et*

al, 2013). However, ultraviolet radiation also promotes human health by facilitating the natural synthesis of vitamin D (Mo *etal,* 2025) and endorphins in the epidermis (Kim *etal,* 2023); consequently, UV exposure has both beneficial and detrimental effects on human health. Nonetheless, excessive exposure to ultraviolet radiation poses significant health risks, including tissue atrophy, pigmentary alterations, wrinkles, and malignancies (D'Orazio *et al.,* 2013).

The primary source of UV radiation is solar radiation, also known as sunlight (Gallagher *et al,*2010). As a segment of the electromagnetic spectrum, ultraviolet photons occupy the range between the wavelengths of visible light and gamma radiation (Vollmer, 2021). There are three types of UV radiation: Ultraviolet A (UVA), Ultraviolet B (UVB), and Ultraviolet C (UVC), which differ in wavelength and penetration according to their electro-physical properties (Mohania *et al,* 2017; Hamouda *et al,* 2022). UV-C photons possess the shortest wavelengths (100-280 nm) and the highest energy, while UV-A photons have the longest wavelengths (315-400 nm) and the lowest energy, with UV-B occupying the intermediate range (280-315 nm). Each component of ultraviolet radiation can influence cells, tissues, and molecules in diverse ways (Mohania *et al,* 2017).

Moreover, due to air ozone that absorbs UVC, ambient sunlight primarily consists of UVA (90%-95%) and UVB (5%-10%). Ultraviolet radiation penetrates the skin in a wavelength-dependent manner (Welch *et al,*2022). Longer wavelength UVA penetrates deeply into the dermis, reaching significant depths (Finlayson *et al,* 2022). UVA effectively produces reactive oxygen species that can harm DNA through indirect photosensitizing mechanisms (Brem *et al,* 2017). Conversely, UVB is predominantly absorbed by the epidermis, with minimal penetration into the dermis (Reich & Medrek, 2013). UVB has the most direct impact on epidermal cells due to its limited penetration depth and strong absorption by nucleic acids, proteins, and endogenous chromophores (Song *et al,* 2025). It is directly absorbed by DNA, which induces molecular rearrangements, creating specific photoproducts, such as cyclobutane dimers and 6-4 photoproducts (Shakeel *et al,* 2025). Mutations and cancer may arise from numerous alterations to DNA.

Furthurmore, UVB radiation generates a range of photochemical and physiological responses in the skin, including DNA photolesions, oxidative stress, and modulation of immunological function (Gromkowska-Kepka *et ah,* 2021). Due to the epidermis absorbing the bulk of UVB photons, compounds inside this layer, including UCA, undergo direct photochemical changes when exposed to sunlight (Gibbs *et ah,* 2008). UCA, which was generated from histidine metabolism in the epidermis, is a significant UV-absorbing chromophore in the stratum corneum (Ali Mua *et ah,* 2025). UVB irradiation transforms *trans-UCA* to its *cis* isomer through photoisomerization (Peltonen *etah,* 2014), a mechanism that has been well characterized and connected to downstream immunological consequences

2.4 Metabolic Pathway of O^UCA

The outermost layer of skin naturally contains UCA, an important intermediary in histidine metabolism. The histidase enzyme catalysed the deamination process from L-histidine to produce *trans-UCA* as the main product (Norval, 2001). Histidine decarboxylase catalyzes the conversion of histidine to histamine via an enzymatic route, whereas this activity occurs independently (McLoone *etah,* 2005).

Upon exposure to UV radiation, *trans-UCA* undergoes dose-dependent photoisomerization into *cis-UCA* (Peltonen *etah,* 2014). The transition impacts UCA's immunomodulatory properties, which affect skin inflammation and immunological function. The primary metabolic fate of *cis-UCA* involves its conjugation with GSH, catalysed by GST, forming GS(CIE) and leading to the formation of a Cys (CIE). The hydrophilicity of these molecules is increased by these alterations, allowing excretion through sweat and urine (Kinuta *et ah,* 2003). Upon exposure to UV radiation, the UCA, in its *trans-UCA* form, converts to the *cis-UCA* form in a dose-dependent manner (McLoone *etah,* 2005). The metabolic pathway of *cis-UCA* is outlined in Figure 2.3.

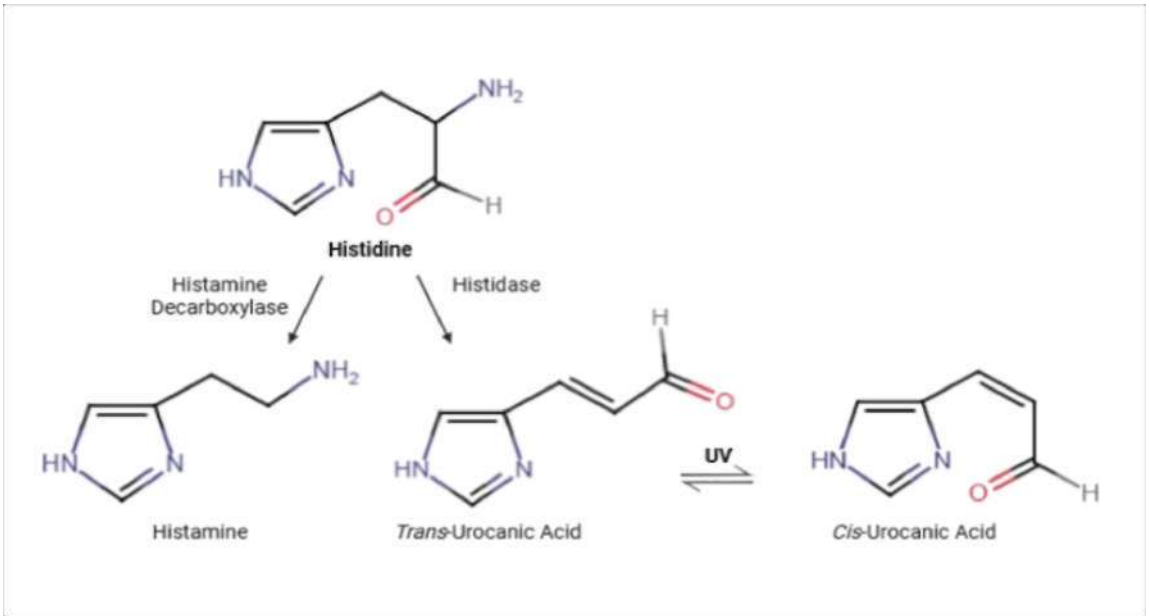

Figure 2.3 The Metabolic Pathway of UCA in the Skin was Generated using RCSB.org

Furthermore, the reaction between *cis*-UCA and RSS was discussed in a 2001 research paper by Kinuta *et al*. In the experiment, they discovered the conjugation of GSH and *cis*-UCA molecule in rat liver in the presence of GST. This was then further analysed, and they concluded that Cys(CIE) can be formed by the GS(CIE) degradation process, which causes this to be excreted in the urine. In addition, the adduct of L-cysteine, S-[2-carboxy-1-(1H-imidazol-4-yl) ethyl]-L-cysteine (Cys(CIE)), was successfully isolated from human urine. This compound was the same as that formed from the GS(CIE) degradation (Kinuta *et al.*,2001). The metabolism pathway of *cis*-UCA involves the conjugation of *cis*-UCA with glutathione (GSH) through the catalysis of glutathione-S-transferase (GST). This results in the further degradation of *cis*-UCA to form a *cis*-UCA-cysteine conjugate (CysSH), which renders the compound polar and facilitates its rapid excretion from the body via sweat and urine (Kinuta *et al*., 2003), as shown in Figure 2.4.

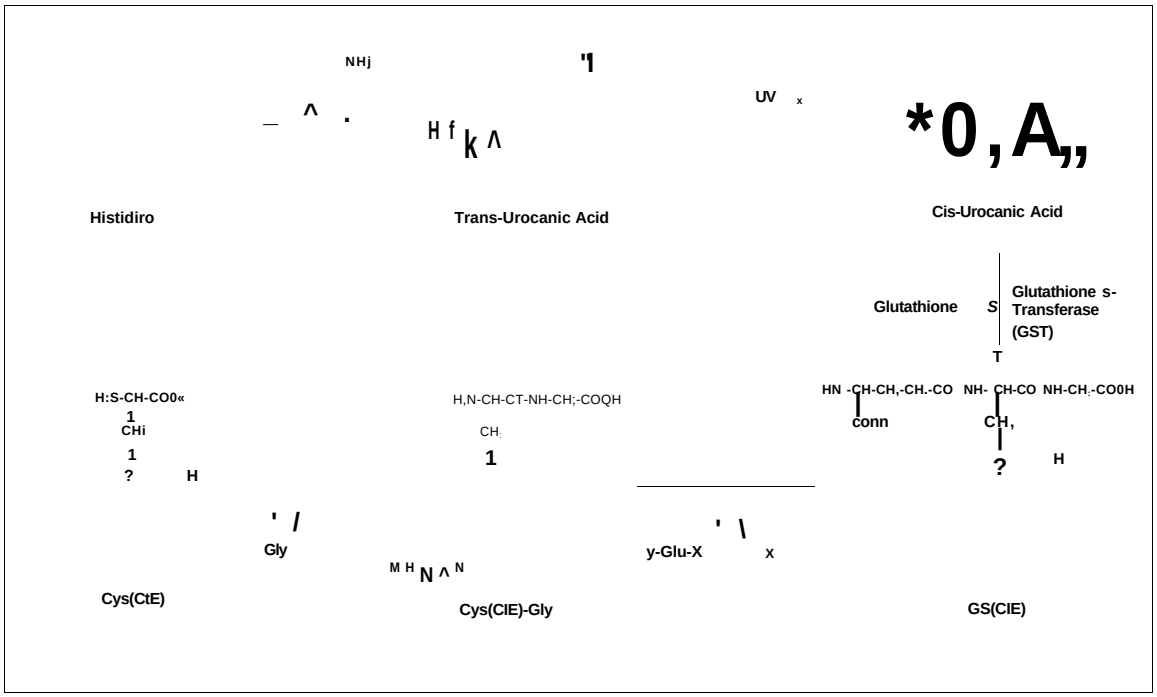

Figure 2.4 The Metabolism Pathway of *Cis-XJCA* was Generated using RCSB.org

2.5 Photobiology of O^UCA

The photobiology of *cis-XJCA* is complex, with both protective and harmful effects depending on its quantity, epidermal location, and the redox state of the surrounding microenvironment. As a UVB photoproduct, *cis-XJCA* absorbs ultraviolet photons in the 300-310 nm range and can release some of the absorbed energy harmlessly as heat, thereby decreasing the penetration of potentially harmful UV photons into deeper skin layers (Gibbs *et ah*, 2008). This suggests a potential photoprotective role under controlled physiological conditions. However, excessive or prolonged accumulation of *cis-UCA*, particularly in chronically UV-exposed skin, has been related to phototoxic and immunosuppressive effects (Hart & Norval, 2018). Table 2.1 shows a summary of the possible protective and harmful effects of *cis-XJCA*.

Table 2.1

Possible Protective and Harmful Effects of *Cis-UCA*

Category	Effects	Description	References
Possible Protective Effects of cis-UCA	Photo-transmitter or photoreceptor role	Acts as a UVB-responsive chromophore influencing phototransduction signalling in the skin; it may fine-tune adaptive photobiological responses.	(Norval e/a/., 2002)
	Anti-inflammatory modulation (context-dependent)	Reduce excessive inflammatory signalling and dampen cytokine overactivation.	(Gibbs & Norval, 2011)
	Homeostasis regulation	Maintaining barrier homeostasis within the stratum corneum.	(Norval *et al.*, 2002)
Possible Harmful Effects of cis-UCA	Phototoxic and immunosuppression	Suppresses Langerhans cell activity, T-cell responses, and systemic immunity following exposure to UVB radiation.	(Norval *et al.*, 2008; Gibbs e/a/., 2008)
	Contribution to UV-induced immunosuppression	Primary mediator linking UVB exposure to downstream immunosuppression.	(De Fabo & Noonan, 2002)
	Interaction with inflammatory / stress pathways	Triggers cytokine-dependent suppression pathways (e.g., TNF-a mediated Langerhans cell depletion).	(Gibbs & Norval, 2011)

At low physiological concentrations, *cis-UCA* has been shown to affect immunological responses by changing cytokine secretion patterns, decreasing contact hypersensitivity, and regulating epidermal Langerhans cell density and function (Norval *etal,* 2008; Gibbs *etal,* 2008). However, at higher concentrations or after continuous UV exposure, *cis-UCA* can increase oxidative stress, promote the persistence of UV-induced DNA lesions, and reduce the effectiveness of nucleotide excision repair mechanisms (Damian *et al.,* 1997; Mooney *et al.,* 2020).

Photoisomerization of the *cis-UCA* is reversible, and the radiation dosage does not affect it. However, the urocanase enzyme, which is responsible for the degradation of UCA, is only present in the liver and brain (Zhu *etal.*, 2018). The lack of this enzyme in human skin results in the accumulation of *cis-UCA* following exposure to UV (Hart & Norval, 2021a; Vieyra-Garcia & Wolf, 2021). *Cis-UCA* is primarily eliminated through urine and sweat, with peak levels occurring 5 to 12 hours after exposure to UV radiation and persisting in the body for 8 to 12 days (Kammeyer *et al.,* 1997).

UCA plays a significant role as a potent UV-absorbing compound in the outermost epidermal layer of human skin (Musa *et al.*,2025). Consequently, it has been widely believed that its primary purpose is to serve as aUV filter, safeguarding against DNA damage. Initially, *trans-XJCA* was added to the sunscreen formulas. Nevertheless, daily exposure to UV irradiation with topically applied *trans-XJCA* in mice increased the incidence of UV-induced tumours and the degree of malignancy (Reeve *et al.*, 1989). This might contribute to the immunomodulating effects of *cis-UCA.* Thus, czs-UCA has been linked to skin-related pathological processes, including immunosuppressive effects and changes in cellular antioxidant balance following exposure to UV radiation.

2.6 Pathological Implications of Oy-UCA on Skin

2.6.1 Skin Cancer

UV irradiation has been considered the primary cause of skin pathological conditions, particularly skin cancer (Laikova *et al.*, 2019). Hence, the first UV sunscreen was developed in 1928 to prevent skin cancer. Nevertheless, according to the Canadian Cancer Society's Advisory Committee on Cancer Statistics (2015), despite the introduction of this revolutionary product, there was no substantial decrease in the incidence of skin cancer. Since the mid-1980s, cis-UCA has been traditionally viewed as an immunosuppressive agent that potentially hinders tumor control. This UVB-activated photobiological pathway produces czs-UCA, an immunomodulatory molecule that inhibits normal skin immune signaling and contributes to local immune suppression, potentially hindering tumor control.

Despite UCA being recognized as a UV photoreceptor years ago and its well-documented role in immune suppression, the specific mechanism of action is still unknown. Czs-UCA induces oxidative DNA damage and the expression of genes related to apoptosis, cell growth arrest, and oxidative stress in cultured human keratinocytes (Kaneko *et al,*2011). It inhibits tumor antigen presentation by Langerhans cells and reduces skin tumour incidence in UVB-irradiated mice treated with a czs-UCA-specific monoclonal antibody (Barresi *etal.*, 2011). Studies have shown higher czs-UCA levels

in squamous cell carcinoma biopsies and increased *cis-UCA* production in patients with a history of skin cancer following UVB irradiation (Decara *et ah,* 2008)

Moreover, *cis-UCA* has been linked to the development of UV-induced skin malignancies due to its immunosuppressive properties and interference with DNA damage repair. After UVB exposure, *cis-UCA* accumulates in the stratum corneum and inhibits the activity of epidermal Langerhans cells, which are essential for beginning anti-tumour immune responses (Kaneko *etah,* 2008; Jauhonen, 2017). This suppression is achieved by changes in cytokine profiles, such as increased interleukin-10 (TL-10) and decreased interleukin-12 (XL-12) production, which tilt the immune system toward tolerance rather than tumour surveillance (Damian *et ah,* 1997; Gopal, 2014). Additionally, *cis-UCA* binding to the 5-HT2A serotonin receptor reduces the immune response in mice. The immunosuppression was rescued by blocking the 5-HT2A serotonin receptor (Walterscheid *et ah,* 2006). This finding highlights the mechanism of immunosuppression caused by *cis-UCA* and its potential link to the development of skin cancer.

Additionally, *cis-UCA* can acidify the cytosol of tumor cells, initiating apoptotic pathways and cell death, as demonstrated in melanoma xenografts, bladder carcinoma cells, and urothelial carcinoma models (Laihia *et ah,*2010; Peuhu *et ah,* 2010). *Cis-UCA* also exhibits immune modulation properties, and excessive immune system activation in response to the *cis-UCA* isomerization may influence interleukin production (IL-ip, IL-6), activate matrix metalloproteinases (MMPs), and contribute to inflammatory skin conditions and hypersensitivity reactions, thereby accelerating skin damage (Salminen *etah,* 2022).

Furthermore, *cis-UCA* has been shown to increase the persistence of cyclobutane pyrimidine dimers (CPDs) and other UV-induced DNA lesions by inhibiting nucleotide excision repair pathways, thereby allowing mutant keratinocytes to survive and proliferate (Mooney *etah,* 2020). Skin malignancies caused by persistent UV exposure and prolonged *cis-UCA* activity often exhibit noticeable changes on the skin surface. Common symptoms include the creation of new growths or sores that do not heal, changes in the size, shape, or colour of existing moles, persistent itching or

pain, and the formation of rough, scaly, or crusted lesions. Squamous cell carcinoma lesions may be complex, appearing as red nodules or flat sores with a scaly crust. In contrast, basal cell carcinoma lesions are typically pearly or waxy lumps, flat flesh-coloured lesions, or brown scar-like patches. Melanoma, albeit less prevalent, can appear as irregularly shaped pigmented lesions with colour fluctuation, asymmetry, and changing borders (Johal, Saour, & Mohanna, 2021).

These clinical characteristics are summarised and physically represented in Figure 2.5, which illustrates typical cutaneous symptoms of UV-induced skin malignancies. The graphic can be used as a reference to identify early warning indicators, emphasising the necessity of early detection and intervention. Long-term *cis-XJCA* accumulation in sun-exposed skin may combine with UVB mutagenesis to induce squamous and basal cell carcinoma (Hosseini, 2015), emphasizing the importance of *cis-XJCA* metabolism-targeted preventative measures.

(A) (B) (C)

Figure 2.5 Typical Cutaneous Presentations of UV-Induced Skin Malignancies: (A) Basal Cell Carcinoma Showing a Pearly, Translucent Papule with Telangiectasia; (B) Squamous Cell Carcinoma Presenting as a Firm, Scaly Hyperkeratotic Plaque; and (C) Malignant Melanoma Characterised by Asymmetric, Irregularly Pigmented Lesions (Mayo Clinic,2025).

2.6.2 Skin Allergies (Urticaria and Atopic Dermatitis)

Cis-XJCA has been related to the worsening of allergic skin disorders, including urticaria and atopic dermatitis (AD). This effect is thought to arise from its ability to skew cutaneous immune responses toward a Th2-dominant profile, enhance cytokines such as IL-4 and IL-10, and weaken local immune surveillance, thereby promoting

allergic inflammation in susceptible skin environments (Norval *et al*., 1995; Gibbs *et al*., 2008). The increased levels of *cis*-UCA following UV exposure may exacerbate AD symptoms in some individuals by affecting systemic immune response. Although *cis*-UCA has an immunosuppressive effect, it could also act as a pro-inflammatory factor under specific conditions. Filaggrin deficiency in AD has been shown to reduce *trans*-UCA levels; hence, altered *cis*-UCA activity could disrupt the skin barrier (Pellerin *et al*., 2013).

In experimental models of AD, increasing *cis*-UCA levels have been associated with enhanced mast cell degranulation and histamine release, resulting in erythema, pruritus, and the development of wheals (Gilmour *et al*., 1993). Additionally, *cis*-UCA has been reported to impair epidermal barrier function, allowing for higher allergen penetration and thereby increasing the inflammatory cascade in predisposed individuals (Jauhonen, 2017). Clinical and animal studies have shown that modifying *cis*-UCA levels, either topically or systemically, can affect the severity of AD symptoms, suggesting a direct pathophysiological function (Damian *et al*., 1999). This molecular relationship between *cis*-UCA metabolism and allergic skin illnesses gives vital insight into disease development. It identifies *cis*-UCA as a possible treatment target for inflammatory dermatoses marked by Th2 dominance.

UCA is one of the natural moisturising agents, along with lipids and proteins, that contribute to sustaining the strength of the skin barrier through a complex relationship between them. The skin barrier primarily consists of the stratum corneum, the outermost layer of the epidermis (Chen *et al*.,2024). The presence of this layer is vital in shielding the body from external factors such as environmental stresses, infections, and water loss (Yoo *et al*., 2024). In AD, *cis*-UCA reduces skin inflammation by enhancing the skin barrier and reducing water loss, thereby helping to alleviate symptoms.

However, in chronic spontaneous urticaria, patients exhibit higher concentrations of *cis*-UCA and an increased *cis*-UCA to *trans*-UCA ratio in the stratum corneum, potentially enhancing mast cell degranulation and promoting urticaria symptoms, thereby worsening the condition by triggering an allergic response. This was

supported by evidence of cz's-UCA-induced mast cell degranulation in the skin (Pham *et ah,* 2017). Thus, while *cis-UCA* has therapeutic potential in AD, it may exacerbate urticaria due to its effects on immune cells (Ye *et ah,* 2014).

Clinically, atopic dermatitis is often characterized by chronic eczematous areas with erythema, dryness, excoriation, and lichenification, indicating a recurring and persistent course (Frazier *et ah,* 2020). Urticaria, on the other hand, is characterized by brief wheals, cutaneous edema, pruritus, and erythematous flares, with lesions typically disappearing within hours (Zuberbier *et ah,* 2022). The opposing symptom patterns enable easy visual separation between the two illnesses. The symptoms of these two types of skin allergies, which present with distinct clinical characteristics due to UV, are shown in Figure 2.6.

^

(a) (b)

Figure 2.6 Clinical Presentation of UV-Related Skin Allergies: (A) Atopic Dermatitis, Showing Chronic Eczematous Lesions with Erythema, Dryness, and Lichenification (Frazier *Et Ah,* 2020); and (B) Urticaria, Characterised by Transient Wheals with Dermal Edema and Pronounced Pruritus (Zuberbier *et ah,* 2022).

2.6.3 Photoaging

Cis-UCA is involved in photoaging primarily due to its immunomodulatory properties and its response to UV light (De Fabo & Noonan, 2002). As an early sign of UV-induced damage, *cis-XJCA* is generated when UCA undergoes photoisomerisation. Although immune-suppressive properties are present in *cis-XJCA*, its continuous formation due to repeated UV exposure may contribute to the chronic inflammatory responses observed in photoaging (Salminen *etal.,2022).*

In addition, Kripke *et al* (1992) have also demonstrated that UV radiation induces *cis-UCA* formation, suppressing immune functions in the epidermis. The expression of MMPs, particularly MMP-1, which targets collagen explicitly, is increased, and *cis-UCA* indirectly amplifies the inflammatory response (Feng *et al,*2024). Frequent exposure to UV radiation and ongoing MMP activity weaken the skin's collagen network, causing wrinkles and decreased skin elasticity, ultimately resulting in photoaging (Hussein *et al,* 2025).

There is a notable case published case report by The New England Journal of Medicine in 2012, which shows the clinical representation example of chronic unilateral photoaging shown in Figure 2.7, of on a 69-year-old truck driver whose left side was exposed to UV radiation for more than 25 years Due to extended exposure to UV rays through the driver's side window, the left side of his face had significantly more dermatoheliosis than the right side. The clinical examination revealed thickness, wrinkling, and darkening on the exposed side, consistent with UV-induced skin elastosis (Gordon & Brieva, 2012). This case highlights the cumulative and unequal impacts of UV radiation in workplace situations.

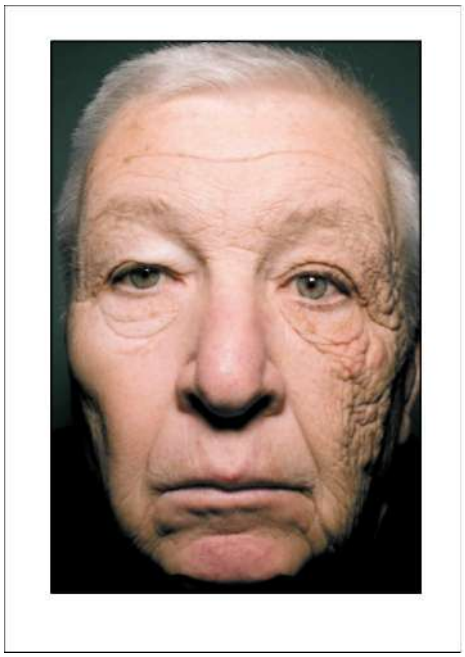

Figure 2.7 The Clinical Representation of Chronic Unilateral Photoaging in a 69-Year-Old Truck Driver with Chronic UV Exposure to the Left Side of the Face for over 25 Years, Demonstrating Marked Photoaging, including Deep Wrinkling and Skin Sagging on the Sun-Exposed Side (Gordon&Brieva,2021).

Additionally, it has been shown that *cis-XJCA* reduces cell viability. Research has shown that *cis-XJCA* alone can enhance the generation of ROS in cells, resulting in oxidative stress and cell damage (Korhonen *et al,* 2023). In addition, Kaneko and her colleagues (Kaneko *et al.,* 2011) conducted a study utilising keratinocytes as a model for their research. They demonstrated that treating normal human epidermal keratinocytes with *cis-XJCA* increased cell mortality. *Cis-XJCA* generates ROS in a dose-dependent manner, but *trans-XJCA* does not.

Exposure to UV radiation leads to increased ROS production, which triggers the activation of MMPs, particularly MMP-1, MMP-3, and MMP-9, resulting in collagen degradation and skin aging (Gromkowska-K^pka *et al,* 2021). Among these, MMP-1 (collagenase-1) specifically breaks down type I and III collagen, reducing skin elasticity and accelerating wrinkle formation (Tirka *et al,* 2023). In addition, oxidative stress markers such as 8-hydroxy-2'-deoxyguanosine (8-OHdG) and malondialdehyde (MDA) are significantly elevated following UV exposure, indicating increased DNA and lipid peroxidation damage, both of which contribute to photoaging (Dong *et al,* 2008). UV radiation also stimulates pro-inflammatory cytokines, such as IL-6 and TNF-a, further

exacerbating chronic inflammation and degradation of the extracellular matrix (ECM) (Zorina *etal,* 2022). These cumulative effects ultimately weaken the dermal structure, increasing the visibility of fine lines and sagging. The key biomarkers involved in UV-induced photoaging, along with their functions, are summarized in Table 2.2.

Table 2.2
Key Biomarkers Associated with UV-Induced Photoaging

Biomarkers	Functions	Impacts on Photoaging	References
MMP-1 (Collagenase-1)	Breaks down type I and III collagen	Loss of skin elasticity, wrinkle formation	(Feng *et al.* ,2024)
MMP-3 (Stromelysin-1)	Degrades elastin and proteoglycans	Weakens the ECM, causing sagging skin	(Feng *et al.* ,2024)
MMP-9 (Gelatinase B)	Degrades type IV collagen	Contributes to skin thinning and fragility	(Feng *et al.* ,2024)
8-Hydroxy-2'-deoxyguanosine (8-OHdG)	Marker of DNA oxidation	Indicates UV-induced DNA damage and accelerated ageing	(Loyokuni *et al,* 2011)
Malondialdehyde (MDA)	Lipid peroxidation marker	Reflects oxidative stress-induced skin damage	(LiPomi.,e/a/.,2025)
IL-6, TNF-a	Pro-inflammatory cytokines	Promote chronic inflammation and ECM degradation	(Ansary *etal.,2021)*

2.7 Therapeutic Potential of c/y-UCA

2.7.1 Natural UV Filter

Cis-XJCA is an endogenous molecule that absorbs UV light and acts as a sunscreen. It has been identified as a potential natural UV filter due to its ability to absorb UVB rays in the 300-310 nm range and dissipate the energy as heat (Gibbs *et al,* 2008; Norval & El-Ghorr, 2002). This characteristic reduces UV penetration into deeper epidermal layers, minimizing DNA damage and oxidative stress in keratinocytes. Unlike synthetic sunscreens, *cis-XJCA* is an endogenous metabolite in the stratum corneum, which may give superior biocompatibility and decreased allergic risk (Jauhonen, 2017). Human *in vivo* investigations have assessed *cis-XJCA* levels in the skin and revealed their fluctuation with UV exposure (McLoone *etal,* 2005; Egawa *et*

al, 2010). Although topical supplementation could theoretically increase photoprotection, excessive *cis-XJCA* may promote immunosuppression (Mooney *et al.,* 2020). This dual nature underlines the need for dose-controlled application techniques.

According to Peltonen *et al* (2014), its capacity to absorb and disperse UV rays increases the possibility of its use in topical photoprotective compositions. Verma *etal* (2024) stated that before *cis-XJCA* is used in medical applications, its contradictory role in UV-related cancer risk must be considered. On the other hand, *cis-XJCA* can effectively reduce acute and subacute skin inflammation, outperforming hydrocortisone and tacrolimus in mouse models by decreasing skin irritation, oedema, and erythema without affecting neutrophil infiltration or epidermal thickness (Jauhonen, 2017). *Cis-XJCA* has been implicated in the pathogenesis of photosensitivity reactions (Hart & Norval, 2021a).

However, a recent study has shown that *cis-XJCA* can serve as a photodynamic agent with potential anti-inflammatory and antiproliferative activity (Laihia *et al.,* 2010). In addition, two natural UCA derivatives, imidazole-4-carboxylic acid (ImCOOH) and imidazole-4-acetic acid (ImAc), were found to have an excellent safety profile after the preclinical test phase, including partial systemic exposure through skin penetration (Kammeyer *etal.,* 2012).

2.7.2 Cancer Therapy

Beyond dermatology, *cis-XJCA* and its derivatives have garnered attention in oncology due to their ability to influence the tumor microenvironment. Certain synthetic analogues have been demonstrated to affect extracellular pH, reduce pro-inflammatory cytokine production, and increase immune cell infiltration into tumours (Arentsen *et al.,* 2012). These actions may increase cancer cell sensitivity to chemotherapeutic drugs and immune-mediated clearance. In murine cancer models, *cis-XJCA* therapy has been linked to decreased tumour development and improved survival rates (Laihia *et al.,* 2010). In cutaneous cancers, its ability to control UV-induced DNA repair pathways could be used to selectively sensitize tumour cells to targeted therapy. Clinical translation necessitates a comprehensive evaluation of the therapeutic window, the

optimal dose, and delivery mechanisms to prevent systemic immunosuppression or unexpected tumor tolerance.

Upon intravesical instillation of *cis*-UCA, this agent is protonated at the imidazolyl moiety in the mildly acidic extracellular tumour environment and penetrates the cancer cell. Once inside the cell, due to the slightly alkaline pH inside the tumour cell, *cis*-UCA is deprotonated, i.e., the imidazolyl proton is released into the cytosol, which increases the intracellular acidity. This acidification impairs many cellular processes, such as metabolic activity, and may lead to cell cycle arrest, induction of cellular apoptosis, and necrotic cell death (Peuhu *et al*., 2010). Moreover, new research has demonstrated that *cis*-UCA affects important intracellular signalling pathways, specifically the c-Jun N-terminal kinase (JNK) and extracellular signal-regulated kinase (ERK) mechanisms. A significant component of the mitogen-activated protein kinase (MAPK) cascade, the ERK pathway plays a role in cell survival, differentiation, and proliferation (Laihia *et al*., 2010). Although ERK activation stimulates cell development, sustained phosphorylation of ERK (p-ERK) in malignant cells can result in uncontrolled proliferation. Studies indicate that *cis*-UCA suppresses ERK phosphorylation, leading to cell cycle arrest and inhibition of tumour growth (Laihia *et al*., 2010).

The JNK pathway, on the other hand, is typically associated with cellular stress responses, particularly apoptosis. It has been demonstrated that *cis*-UCA increases JNK activation in tumour models, which upregulates pro-apoptotic proteins such as caspase-3 and Bax, promoting programmed cell death (Peuhu *et al*., 2010). This implies that *cis*-UCA might selectively target cancer cells while protecting healthy tissues by acting as an apoptotic inducer. The exciting potential of *cis*-UCA as an anti-cancer therapy is highlighted by its simultaneous control of ERK (inhibition) and JNK (activation), especially when combined with targeted therapies that exploit tumor weaknesses. However, more research is required to determine the ideal treatment parameters, such as dosage, formulation, and delivery methods, to optimise *cis*-UCA's anti-tumour effectiveness and minimise its off-target effects.

2.7.3 Skin Barrier Function

Cis-UCA helps maintain epidermal barrier homeostasis by regulating the acidic pH of the stratum corneum, which is crucial for the activity of lipid-processing enzymes, ceramide formation, and corneocyte desquamation (Pham *et ah,* 2017; Gibbs *et ah,* 2008). Acidic pH limits pathogenic bacteria development and promotes the skin's antimicrobial defence. The skin's pH is raised in disorders such as atopic dermatitis and xerosis, hindering barrier repair. Restoring *cis-XJCA* levels could help re-acidify the stratum corneum and improve barrier function (Choi *et ah,* 2023; Lukic *etah,* 2021).

Cis-UCA is crucial for maintaining the integrity of the skin barrier. Reduced *trans-XJCA* levels in filaggrin-deficient skin have been found to cause problems with skin hydration and pH balance, which can worsen diseases like chronic eczema and AD (Tan *et ah,* 2017). In AD patients, impaired barrier integrity and skin hydration were noted due to reduced levels of natural moisture factor amino acids, including histidine and UCA (Moosbrugger-Martinz *et ah,* 2022). Randomized, double-blinded, vehicle-controlled clinical trial, treatment with a 5% *cis-XJCA* cream reduced transepidermal water loss and erythema, and thus improved skin barrier function and suppressed inflammation in the human skin with mild and moderate AD (Peltonen *et ah,* 2014). Filaggrin in the stratum corneum is the primary source of UCA.

An alternative approach involving L-histidine supplementation increased filaggrin production and improved skin barrier function, resulting in a 40% reduction in AD severity in patients (Tan *et ah,* 2017). The genetic mutations leading to reduced *trans-XJCA* production might have evolved to allow better synthesis of pre-vitamin D with less UV radiation filtering in lighter skin (Tan *et ah,* 2017). Thus, cz's-UCA-based treatments may help restore filaggrin metabolism, indicating a potential new therapeutic option for chronic dry skin problems. However, excessive *cis-XJCA* may generate immunosuppressive adverse effects; therefore, therapeutic use would require a precise dose.

2.7.4 Immune Modulation

Cis-UCA has been widely studied for its immunomodulatory properties, particularly in AD, psoriasis, and other inflammatory skin diseases. Research has shown that topical *cis-XJCA* reduces inflammatory cytokines, including IL-ip and TNF-a, thereby mitigating skin inflammation (Moosbrugger-Martinz *etal,* 2022). Modulating UCA isomer concentrations in diseased skin may offer therapeutic benefits for controlling inflammation and treating cutaneous disorders like AD. The use of topical *cis-XJCA* resulted in the enhancement of macroscopic features of AD-like skin lesions and a reduction in the level of serum IgE in AD model mice, as reported by Rieko and Motonobu in 2016 (Rieko & Motonobu, 2016).

cis-XJCA is recognized as a significant photoisomerization product of *trans*-UCA in the epidermis following UV exposure, possessing substantial immunomodulatory capabilities that influence both local and systemic immune regulation. *Cis-XJCA* is well-documented for its capacity to produce antigen-specific immunosuppression, particularly by inhibiting delayed-type hypersensitivity and contact hypersensitivity responses (Wei, 2019; Gibbs *et al,* 2008). *Cis-XJCA* has been demonstrated to modulate cytokine profiles by downregulating pro-inflammatory mediators, including IL-ip, TNF-a, and interferon-gamma (IFN-y), while concurrently promoting anti-inflammatory cytokines such as IL-10 (Norval & Halliday, 2011; Feng *et al,* 2024). The immunosuppressive effect is partially facilitated through its engagement with histamine H2 receptors on Langerhans cells and keratinocytes, leading to modified antigen-presenting cell functionality and diminished migration to draining lymph nodes (Damian *et al,* 1999; Walterscheid *et al,* 2002). Moreover, recent findings suggest that *cis-XJCA* may modulate the function of regulatory T cells (Tregs), promote peripheral tolerance, and mitigate excessive immunological activation (Jimenez-Sanchez *et al,* 2025). These qualities have garnered attention for using *cis-XJCA* and its analogues as prospective treatments in hyperactive immune responses, including autoimmune skin diseases, graft-versus-host disease, and chronic inflammatory disorders (Hart *et al,* 2019). The dual nature of its immunomodulatory effects, protecting against detrimental inflammation while potentially hindering immune surveillance against malignancies and pathogens, requires meticulous assessment in practical applications (Norval & Halliday, 2011).

Additionally, UVB exposure increases the formation of *cis-UCA,* which interacts with serotonin receptors, particularly the 5-HT2A receptor. This neuro-immune signalling pathway may contribute to UVB-induced skin changes, including altered inflammation, vasodilation, and local immunosuppression (Walterscheid *et ah,* 2006). These could potentially lead to novel treatment strategies for treating human AD using topical *cis-UCA.* Interestingly, a study by Hamid *etal.* (2023) demonstrated that RSS can protect keratinocyte cells from UV-A but not UV-B irradiation. The study further revealed that the cooperative interaction of RSS and *cis-UCA* may potentially suppress UV-B-induced inflammation and cellular damage. This can be significant in skin health, as UCA is primarily found in the skin and plays a role in regulating immune responses in the skin (Yu, 2016). Further investigations into the role of *cis-UCA* in inflammatory pathways may provide insights into new dermatological treatments.

2.8 Reactive Sulphur Species (RSS)

Reactive Sulphur species (RSS), also known as super sulphides, are a highly reactive chemical form of sulphur. They are important biological mediators and play key roles in different pathophysiological conditions (Bolton *etal.,* 2020). They possess unique chemical properties distinct from those of their thiol counterparts, making them reactive and capable of participating in redox signalling (Kasamatsu & Ihara, 2021). This diverse family of sulphur-containing molecules plays a crucial role in redox regulation, cellular signalling, and protection against oxidative stress (Iciek *et ah,* 2022). RSS modulates protein function through sulphuration, which is a chemical process in which a sulphur-containing group is added to a molecule that readily contains a carbon chain and protects against oxidative and electrophilic stress by reacting with ROS and electrophiles (Kolluru *etal.,* 2020; Iciek *et ah,* 2022).

RSS is a crucial precursor for metabolic processes within the body (Bilska-Wilkosz & Iciek, 2022). As the name indicates, RSS contains sulfur, and on average, the human body contains approximately 14mg of sulfur per kilogram (Anastassakis, 2022). Some examples of active thiol compounds in the body are cysteine (Cys), homocysteine (Hey), and lipoic acid (Francioso *et al,* 2020). Lipoic acids could be further divided into a few molecules, one of which is reduced glutathione. In the tissue,

these thiol compound can exist in free and bound form. While bound to protein, they can also undergo reduction and oxidation. (Prakash *etal,* 2009).

GSH is also an antioxidant, one of the most naturally occurring antioxidants in the human body (Hristov, 2022). When oxidative stress occurs in the cell, GSH is one of the free radical scavengers that limit the oxidative damage in the cell. GSH can exist in two forms: the reduced glutathione and oxidized glutathione, commonly known as GSSG. The biological system maintains a high ratio of GSH: GSSG (>100:1) under normal conditions. GSH acts as a protective agent of the system by oxidizing itself to GSSG, rather than other cell components. This GSSG is then converted back into the reduced form, GSH, to maintain the redox homeostasis of thiols (Sadhu *etal,* 2017). It was also found that when there is a high level of GSSG in the cell, it is under oxidative stress because a large amount of glutathione is being oxidized, as many as ROS are available.

Mechanistically, based on recent research by Hamid *et al.* (2023), RSS may interact with the electrophilic double bond of *cis-XJCA* through thiol-based conjugation or redox buffering, thereby lowering ROS production and subsequent inflammatory signaling in keratinocytes. Therefore, it is hypothesised that the cz's-UCA-CysSH conjugation is just one of many by-products in *cis-XJCA* metabolism, and this potentially further discovers varieties of cz's-UCA-sulphide conjugation due to the interaction of *cis-XJCA* and super sulphides. Moreover, *cis-XJCA* has a significant role in UV-induced immunosuppression by initiating gene transcription in keratinocytes, including genes involved in oxidative stress response, cytokine production, and inflammation regulation (Kaneko *etal,* 2008). *Cis-XJCA* also induces oxidative stress-related genes and lipid peroxidation, activating redox-sensitive transcription factors such as NF-KB, which also respond to changes in cellular redox state modulated by RSS (Kolluru *etal,* 2023). Through their nucleophilic and antioxidant properties, RSS may modulate the oxidative environment in keratinocytes affected by *cis-XJCA,* potentially influencing the extent or nature of gene expression changes triggered by *cis-XJCA* (Kaneko *et al,* 2008).

Super sulphides are compounds or molecules with extra sulphur atoms catenated in thiols and proteins, rendering their nucleophihcity proportional to the number of sulphur atoms. It has been found that our body contains an abundance of organic super-sulfides, such as CysSSH and GSSH, which play significant physiological roles (Akaike *et ah,* 2017). A recent study revealed that protein-rich foods such as meat and beans contain many super sulphides, indicating that humans can easily obtain an exogenous supply of super sulphides from our diet (Kasamatsu *et ah,* 2024). Although several super sulphides have been identified and their role in disease control has been outlined, their biological properties are still mostly unknown (Barayeu *et ah,* 2023). Understanding of RSS biology has therapeutic potential, with research focusing on developing sulphide donors and controlled delivery systems to modulate their levels for treatment purposes (Pandey *et ah,* 2024; Lu *etah,* 2023; Khaodade *et ah,*,2023).

2.9 Glutathione-S-Transferase

Glutathione S-transferases (GSTs) are a superfamily of phase II detoxification enzymes primarily found in the cytosol of eukaryotic and prokaryotic cells (Shehu *et ah,* 2019). They catalyse the conjugation of the tripeptide glutathione (GSH) to a wide variety of electrophilic substrates, facilitating their detoxification and excretion by increasing their water solubility (National Centre for Biotechnology Information, 2025). This enzyme plays a crucial role in catalyzing the formation of thioether bonds between the cysteine residue of GSH and electrophilic centres on substrates, resulting in less reactive, more water-soluble conjugates that can be excreted via bile, urine, or sweat (Oakley, 2011). GSTs also interact with signaling molecules, such as c-Jun N-terminal kinase (TNK1) and apoptosis signal-regulating kinase (ASK1), influencing mitogen-activated protein kinase (MAPK) pathways that control cell survival and apoptosis (Sciskalska *etah,* 2020).

The GST enzyme catalyzes the conjugation of *cis-XJCA* with GSH in the *cis*-UCA metabolism pathway. This conjugation forms a cz's-UCA-glutathione conjugate, which is metabolized to a Cys(CIE). This conjugation increases the hydrophihcity of *cis-XJCA* metabolites, facilitating their excretion through sweat and urine, thereby contributing to the clearance of potentially reactive or immunomodulatory compounds from the skin (Norval *etah,* 2008). This GST-mediated conjugation is a key step in the

detoxification and metabolic processing of *cis-UCA* in the skin, linking GST enzymatic activity directly to the regulation of UV-induced skin responses and immune modulation (Musa *etal.,* 2025).

2.10 Analytical Method: Nuclear Magnetic Resonance (NMR) Spectroscopy

Nuclear Magnetic Resonance (NMR) spectroscopy is a commonly used analytical technique for characterizing small molecules, metabolic intermediates, and reaction products based on the magnetic behavior of atomic nuclei (Bothwell & Griffin, 2011). In metabolomic research, NMR gives rich structural information without requiring derivatisation or substantial sample preparation, making it particularly useful for detecting small chemical alterations, such as conjugation events or thiol additions (Nagana Gowda *etal.,* 2022). Because NMR directly detects the chemical environment of hydrogen (^{1}H) and carbon (^{13}C) nuclei, it enables exact identification of shifts in functional groups and can discriminate between isomeric or structurally similar molecules (Salah, 2025)

In addition, due to its ability, NMR can directly detect changes in the magnetic surroundings of nuclei, and it is highly sensitive to variations in functional groups, such as carboxyls, imidazole rings, and thiols (Li *et al.,* 2022). This makes it excellent for recognizing chemical shift changes that occur during conjugation processes, notably those involving reactive sulphur species (RSS). In the context of this investigation, NMR was employed to identify possible cz's-UCA-RSS compounds formed in a cell-free system. Its high precision, repeatability, and non-destructive nature enabled confident detection of structural modifications (Emwas *etal.,* 2020) and encouraged the discovery of new chemicals that may participate in alternate *cis-UCA* metabolic pathways. Thus, NMR serves not only as a structural confirmation technique but also as a vital component in revealing the chemical interactions (Yadav, 2018) that support the suggested mechanistic model of *cis-UCA* metabolism.

CHAPTER 3
RESEARCH METHODOLOGY

3.1 Experimental Design

This study focuses on a cell-free experimental system, *in silico* analysis, and an *in vitro* study. Together, these methods provide an in-depth and comprehensive exploration of the subject matter, thereby enhancing the validity and impact of the research findings. Figure 3.1 provides a flowchart that outlines these methods by phase. Phase 1 involves a cell-free reaction, followed by phase 2, which is a molecular docking study, and the final phase is an *in vitro* study. Below are a visual representation and a more precise illustration, providing a clearer understanding of the systematic approach adopted in this study.

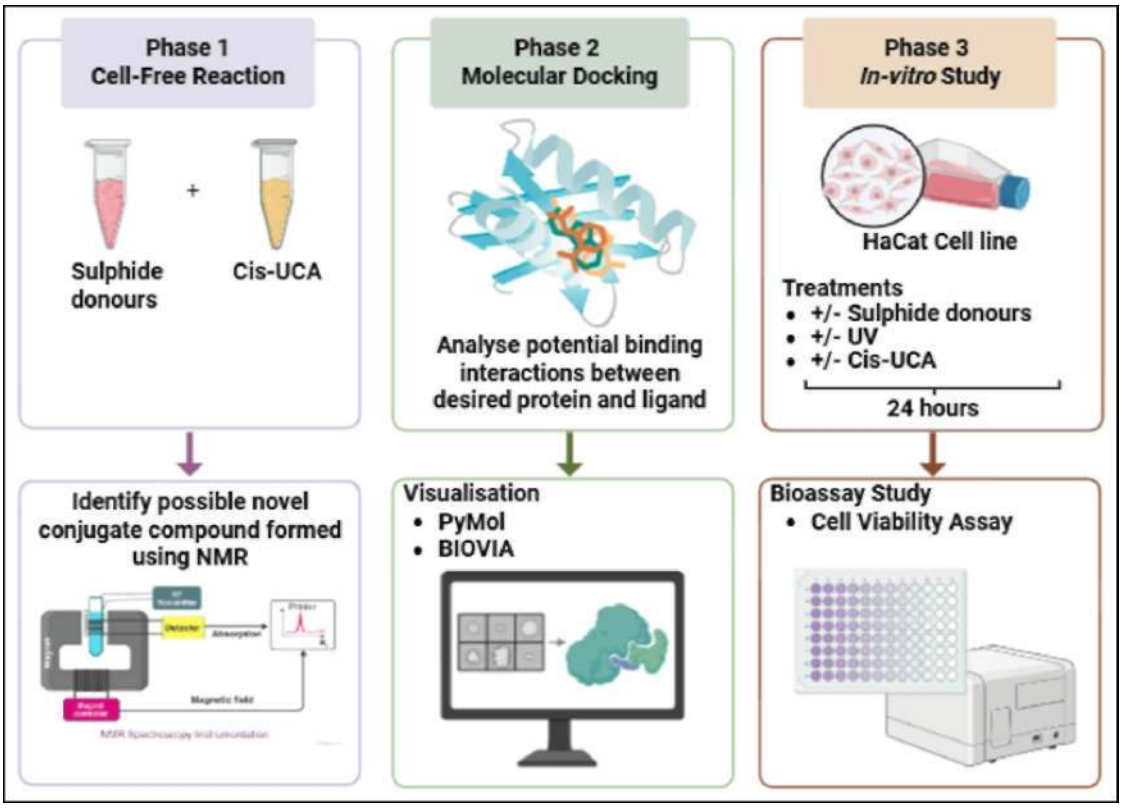

Figure 3.1 Flowchart Outlining Research Methodologies

3.2 Materials and Reagents

Disodium disulfide (Na2S2) was bought from Dojindo Molecular Technologies Inc. (Japan). Sodium hydrogen sulphide (NaHS) reduced glutathione (GSH), L-Cysteine and N-acetyl cysteine (NAC), cz's-urocanic acid *(cis-XJCA),* and Bruker® NMR tubes obtained from Sigma-Aldrich (St Louis, USA). Dulbecco's Modified Eagle Medium (DMEM) phenol red-free and trypsin were purchased from Nacalai Tesque (Kyoto, Japan). A mixed penicillin-streptomycin solution and fetal bovine serum (FBS) were bought from Gibco (Rockville, MD, USA). NMR solvents, including deuterated methanol, deuterated water, deuterated chloroform, and deuterated acetone, were obtained from Merck (Germany). All solvents purity is 99.8% and are suitable for NMR spectroscopy.

3.3 Instruments

The UV box with UVB dose 10 mJ/cm^2 was calculated by a calibrated UV irradiance photometer (UV-340B, Sampo Scientific Instrument Co. Ltd., Shenzhen). Samples were examined using state-of-the-art solution-state NMR and 1H spectroscopy, analysed using a Bruker 600 MHz Avance III NMR spectrometer (Varian Inc., Palo Alto, Calif). The bioassay study was conducted sterily using a biosafety cabinet, hemocytometer, inverted microscope, and TECAN infinite M200 microplate reader.

3.4 Cell-Free Reactions

In this experiment, the *in vitro* biochemical reactions were performed to predict the possible conjugation of *trans-XJCA* or *cis-XJCA* with the sulphide donors in a cell-free system. The sulphide donors used in this experiment were glutathione (GSH), N-acetylcysteine (NAC), L-Cysteine, sodium hydrosulphide (NaHS), and sodium disulfide (Na_2S_2).

3.4.1 Identification of Conjugate Compound

A 1 mg amount of each sulphide donor and 1 mg of either *cis-UCA* or *trans*-UCA were dissolved in 1ml nitrogen-purged ultrapure water. The samples were prepared in a 50 mL centrifuge tube and were kept in the dark to prevent interference from light. The mixture was gently vortexed until complete dissolution was achieved, with sample preparation performed under minimal exposure to air to reduce oxidative degradation. Samples were frozen overnight at -80°C and maintained for a minimum of 12 hours to ensure complete solidification before further processing. Frozen samples were then transferred to a pre-cooled freeze dryer and subjected to lyophilization under reduced pressure, with the condenser temperature maintained at a temperature of < -50 °C, for 24-48 h, until complete solvent removal was achieved. Upon completion of freeze-drying, the chamber was backfilled with dry nitrogen, and the resulting lyophilized samples were sealed and stored at -20 °C until further analysis. The freeze-dried samples were subsequently analysed using NMR spectroscopy to identify any novel conjugates formed during the reaction.

3.4.2 ^{J}H Nuclear Magnetic Resonance (NMR) Spectroscopy

All samples were analysed using advanced solution-state NMR techniques. For the $^{!}$H spectroscopy, a Bruker 600 MHz Avance III NMR spectrometer (Varian Inc., Palo Alto, California) was employed to analyse all samples. The spectrometer operated at a frequency of 599.871 MHz and a temperature of 298 K, utilising a multinuclear broadband observation (BBO) probe. The standard NOESYPR ID pulse sequence (RD-90°-tl-90°-ACQ) with 100 ms mixing time and 2s water frequency during a recycle delay was used to suppress the residual HOD signal in the intracellular metabolite extracts. The water-suppressed standard ID Carr-Purcell-Meiboom Gill pulse sequence (RD-90°-(T-1 80°-T) n-ACQ) was used to acquire the 1H NMR spectra of the cell culture medium. 64K data points with 1200 Hz and 128 scans of spectral width with 2.0 s and 1.36 s acquisition time were used to record the free induction decays (FIDs). Before the Fourier transformation, the FIDs were weighed using an exponential function with a 0.5Hz line-broadening factor.

3.4.3 Data Processing

Each ^{1}H NMR was set with a 3.54 min acquisition time, comprising 64 scans and a 20-ppm width. Potential metabolites were identified using HSQC and HMBC of the 2D J-res. The J-res spectrum acquisition time was 50 min 18 s with eight scans per 128 increments for the axis of the spin-spin coupling constant over the spectral widths of 66 Hz and 8 K for the chemical shift axis over the spectral width of 5000 Hz. The HSQC spectra were obtained over the 2 to 14 ppm spectral width and -10 to 190 ppm in the Fl and F2 dimensions, respectively. With a data matrix of 0.3 £ 8,012.8 and 32 scans per 256 increments covering the data point 25141.4 x 8012.8, the total running time was two hours and 47 minutes, with an interscan relaxation delay of 1.0 s.

Subsequently, the HMBC analysis was run for 11 h 26 min. With an interscan relaxation delay of 1.0 s, the experiment consisted of 64 scans per 256 increments, covering a total data set of 30165.9 x 8012.8 points. The TSP internal reference peak was set to 0.00 ppm, and all spectra were Fourier transformed, and baseline adjusted. The 1H NMR spectra were processed with MestReNova 7.1.2 software (Mestrelab Research, Spain). The baseline and phase referencing of all 1H NMR spectra were manually corrected to the TSP signal (8 0.00). In eliminating the water suppression and DMSO signals, the 5 5.2-4.6 and 5 2.8-2.69 regions in the cell extract NMR spectra were excluded. To eliminate the effect of residual water, methanol, DMSO, and ethanol signals, the regions of 5 5.19-4.68, 5 3.37-3.33, 5 2.89-2.58, 5 3.69-3.61, and 5 1.23-1.15 were eliminated. SJJVICA-P + 12.0 (Umetrics, Sweden) was used for multivariate analysis.

Principal component analysis (PCA) was applied to mean-centred data to identify outliers and provide data distribution profiles. Sample classes were modeled by analyzing the orthogonal partial least squares discriminant analysis (OPLS-DA) algorithm using a unit variance-scaled approach. These reduced other biological analytical differences and improved separation caused by group variation. Coefficient plots were generated using MATLAB scripts, including some in-house modifications, and colour-coded by the absolute value of coefficients. Each peak from the OPLS-DA

models of the variable importance in the projection (VIP) values was analysed to determine which variables influenced the spectra distribution among the groups.

3.5 Molecular Docking Analysis

In this method, molecular docking of GST and glutathione conjugate was conducted to explore the potential binding interactions of GST binding affinity and mechanism. To assess the binding characteristics of GST, sulforaphane was used as a reference drug. Sulforaphane inhibits GST activity, making it a suitable control. The docking results between GST and sulforaphane were compared with those between GST and glutathione conjugate. AmDock (Valdes-Tresanco *et al*, 2020) was used for the molecular docking process, and PyMOL (Schrodinger, LLC, 2015) was employed to visualise the docking results. Molecular docking is an automated procedure for predicting the interaction of ligands with the target protein. Steps performed include protein and ligand preparation, identification of the docking region, and the docking process.

3.5.1 Protein and Ligand Preparation

The 3D structure of GST was retrieved from the RCSB Protein Data Bank (PDB ID: 18GS) with a resolution of 1.9 A using X-ray diffraction (Oakley *et al*, 1999). The ligands used in this study were GS(CIE), and sulforaphane as reference drugs. The GS(CIE) was generated using ChemDraw, saved in CDXML, and converted into PDB format with a 3D coordinate file using OpenBabel.com. The structure of sulforaphane (a known GST antagonist) was retrieved from PubChem (CID: 5350).

3.5.2 Identification of Docking Region

The key GST residues involved in binding were identified, including Tyr7, Argl3, Tyrl08, and VallO. These residues are crucial for GST's binding interactions, as reported by several studies (Hayes & Pulford, 1995; Oakley *et al*, 1999). The grid box was created based on the identified binding residues, with coordinates of x:7, y: 12,

z:18 to cover the specific residues involved in binding. The box size was set to 25x25x25 to ensure proper docking and alignment of the residues for accurate analysis.

Docking parameters were created based on the key GST residues involved in ligand binding. Based on the study by Oakley, critical residues such as Tyr-7, Val-10, Arg-13, and Tyr-108 were essential for binding interactions. These residues were selected for further analysis, as they have been previously shown to participate in hydrogen bonding and hydrophobic interactions with ligands in the active site. The coordinates of these identified residues were extracted from the GST protein structure (PDB ID: 18GS). The residues were located in the binding site of GST, and their exact coordinates were used to define the region of interest for the docking simulations.

A grid box was constructed to cover the binding site of GST, specifically encompassing the identified residues to define the docking region. The centre of the grid box was positioned at coordinates (x:7, y: 12, z: 18), corresponding to the identified binding residues of Tyr-7, Val-10, Arg-13, and Tyr-108. The grid box size was set to 25x25x25, ensuring that it covered the entire binding site, allowing the ligand to explore different docking orientations. To ensure complete coverage of the binding site, the grid box was visualised using PyMOL. The box was confirmed to cover the critical residues (Tyr-7, Val-10, Arg-13, and Tyr-108) as shown in Figure 3.2, with sufficient space around these residues to allow for the proper docking of the ligand. This grid box size was chosen to accommodate the entire binding site while allowing flexibility for the ligand to interact with GST.

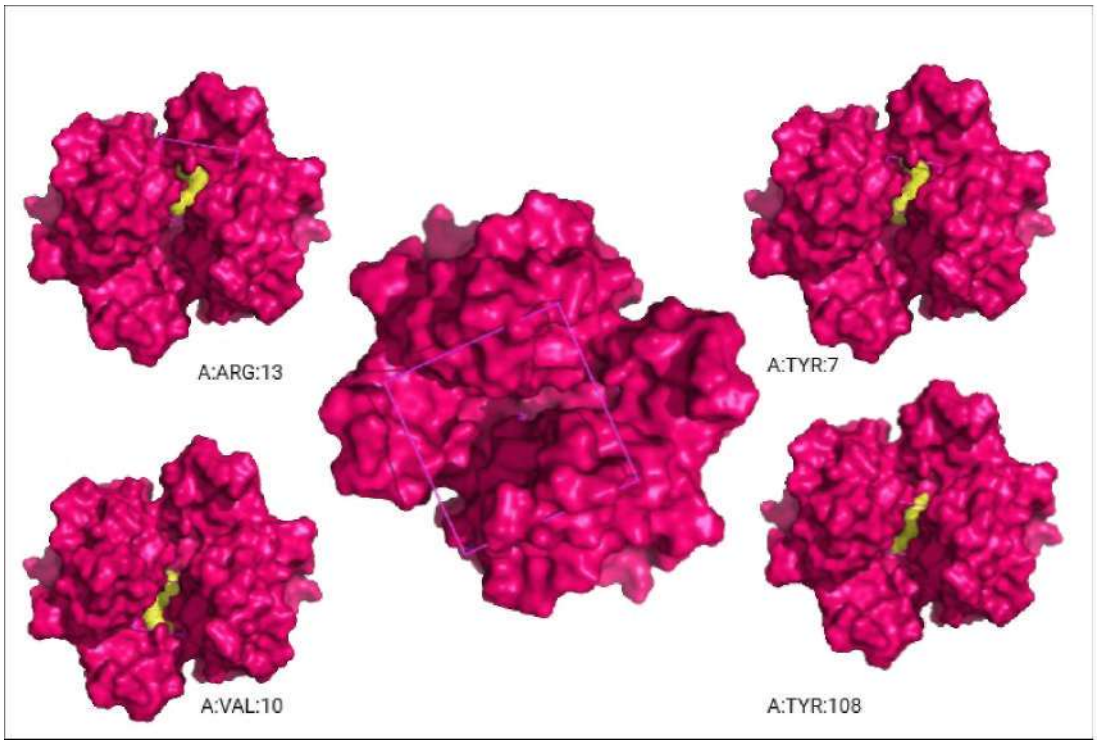

Figure 3.2 The Created Grid Box is Based on the Identified Key GST Residues Involved in the Binding Interaction Generated using Autodock Vina and Visualised using PyMOL

3.5.3 Molecular Docking

The docking process was performed using AmDock Software (Valdes-Tresanco *etal.,* 2020). Pocket docking was performed with the defined grid box with coordinate 7x12x18 within a 25x25x25 size to ensure precision in capturing the interaction between GST and the ligands. Each compound's top-ranked docked conformation was visualised, and its binding affinity was analysed in the docking region of the modelled protein using PyMol (Schrodinger LLC, 2015). At the end of the docking, the polar contacts between the best conformations, based on the docking score, were analyzed for hydrogen bonding interactions, and the residues identified for observation. Then, the molecular docking results were analyzed using a simulation software, Discovery Studio (BIOVIA) v24.1.0.23298 (BIOVIA, 2024), to visualize and identify the varied interactions between the residues of the ligand and its receptor.

3.6 Cell Culture

Human epidermal keratinocytes (HaCaT) cells, at passage number 6, were a gift from the Pharmacology-Toxicology Research Laboratory, Faculty of Pharmacy, Universiti Teknologi MARA (UiTM) Selangor, Puncak Alam Campus, Selangor, Malaysia. Cells were cultured in DMEM high glucose with sodium pyruvate (Nacalai Tesque, Kyoto, Japan) supplemented with 10% bovine calf serum (Gibco, Rockville, MD, USA) and 1% streptomycin-penicillin (Gibco, Rockville, MD, USA). The cells were cultured in a humidified incubator at 37°C with 5% CO2. All work was carried out in a sterilised environment.

3.6.1 Seeding and Treatments

The cells were cultured in a flask until 70%-80% confluence. Then the cells were seeded onto 96-well plates at a density of 1×10^5 cells/well and incubated for 24 hours at 37°C with 5% CO2. After the incubation, the cells were washed with phosphate-buffered saline (PBS) to remove debris. The cells were then pre-treated with 200 uM of various sulphide donors (NaHS, Na2S2, GSH, L-cystine, and NAC) for 3 hours to assess their effect on cell viability. Then the plate was covered in aluminium foil to avoid interference from the ambient light. After pre-treatment with a sulphide donor, cells were treated with 1 mM *cis-XJCA* and/or irradiated with a fluorescent sun lamp (Toshiba FL8BLB, Japan) with emission UVB (320nm, 10 mJ/cm^2) for 18 minutes, placed 22cm above the cell culture flask. The UVB irradiation dose was calibrated using a UV irradiance meter (UV-340B, Sampo Scientific Instrument Co. Ltd., Shenzhen). The irradiation process was performed in the dark to avoid interference from ambient light. Control and experimental groups were conducted as follows:

Groups:

1. Control
2. UVB
3. *cis-XJCA*
4. *cis-XJCA* + UVB
5. Sulphide donor
6. Sulphide donor + *cis-XJCA*

7. Sulphide donor + *cis-UCA* + UVB

After the treatments and/or exposure to UVB irradiation, the cells were incubated in a humidified incubator at 37°C with 5% CO2 for 24 hours.

3.6.2 Cell Viability Measurement (MTT Assay)

After treatment, the cells were subjected to the MTT assay to assess their viability. Fifty microliters of MTT solution were added to each well. Then, the plates were covered with aluminium foil and incubated for 4 hours. Hundred microliters of DMSO were added to each well using a multichannel pipette to solubilise the purple formazan, and the optical density was then read at 490 nm using the Tecan M200 Infinite® Pro Microplate Reader. The cell viability was calculated using the following formula:

$$\textit{Cell viability}\ (\%) = \frac{A(sample) - A(blank)}{A(control) - A(blank)} \times 100$$

Where A(sample) represents the absorbance of the experimental sample, A(control) is the absorbance of the untreated control group, and A(blank) refers to the absorbance of the blank (medium or solvent without cells). All experiments were performed in triplicate, and a p-value less than 0.05 was considered statistically significant. All data were expressed as the mean ± standard error of the mean (SEM)

3.7 Statistical Analysis

All experimental data were analysed using SPSS software version 31. The results were expressed as the mean ± standard error of the mean (SEM). Normality was evaluated with the Shapiro-Wilk test. Student's t-test was applied to compare data from two groups, while one-way analysis of variance (ANOVA) was used to compare more than two groups, and post-hoc Turkey test was performed following a significant ANOVA test. A value of $p<0.05$ was considered statistically significant.

CHAPTER 4
RESULTS

4.1 Oy-Urocanic Acid-Sodium Sulphide Complex and Oy-Urocanic Acid-L-Cysteine Complex

[!]H-NMR data unequivocally demonstrated the complexation between *cis-XJCA*, sodium sulphide, and L-cysteine. The aromatic/heteroaromatic resonances attributed to the imidazole ring are observed in the 8 7.2-8.6 ppm range, while the olefinic (vinylic) UCA signals are detected near 8 6.0-6.7 ppm. These peaks were present in both complexes but exhibited noticeable line broadening and minor chemical shift variations compared to the free ligand, indicative of rapid exchange between the free and metal-bound (or thiolate-bound) states. In the L-cysteine adduct, additional aliphatic resonances (a-CH 8 3.8-4.1 ppm; CH2 8 2.9-3.2 ppm) are observed and are perturbed relative to neat L-Cys, suggesting the involvement of the thiol/thiolate and/or amino group in binding. The absence of the carboxylic proton (D2O solvent) indicates the deprotonation/coordination of the carboxylate in both samples. These data support the formation of 1:1 (or potentially oligomeric) species in rapid exchange, with coordination sites at the imidazole N and carboxylate (and thiolate in the Cys sample).

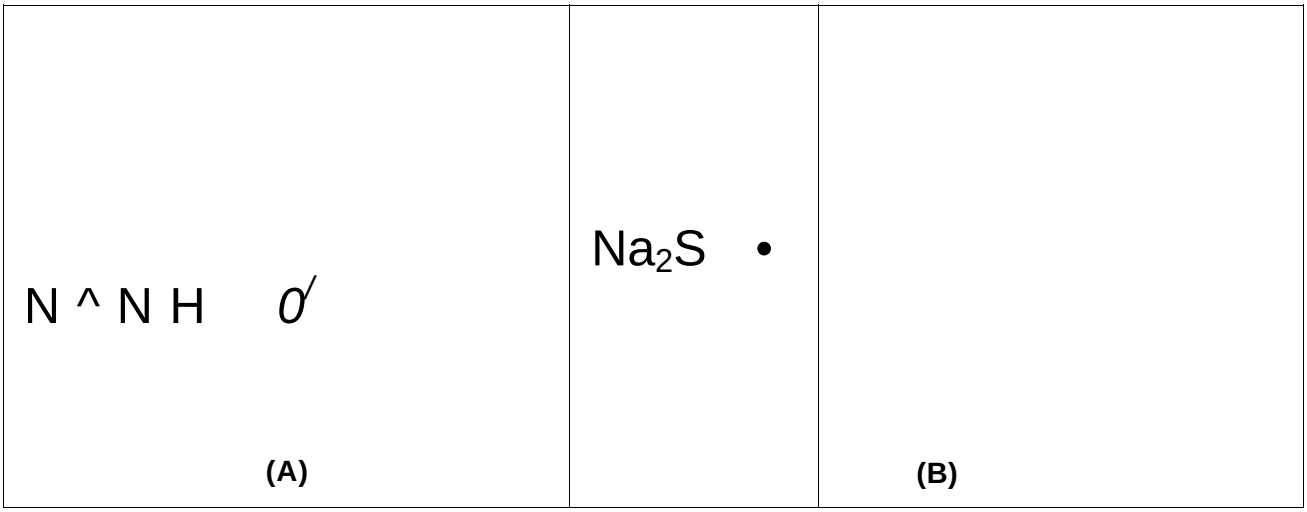

Figure 4.1 Proposed Cz's-Urocanic Acid-Sodium Sulfide Complex was Generated usingRCSB.org

The sodium sulphide sample, an ionic complex or salt, involves the deprotonation of UCA, resulting in the formation of a urocanate anion (-OOC-CH=CH-imidazole). This anion is associated with Na^+ to form sodium urocanate (Figure 4.1 (A)). At the same time, in Figure 4.1 (B), S^{2}~ may function as a counter-ion or as a bridging or ion-paired species, exemplified by [Na^+-UCA^-] andNa2S(UCA~) n aggregates. Coordination or ion pairing at the carboxylate group, along with weak interactions with the imidazole nitrogen, accounts for the observed upfield shifts and line broadening. These proposed chemical structures were shown in Figure 4.2.

There are two potential configurations for the L-cysteine sample:(l) a non-covalent 1:1 complex, wherein the deprotonated urocanate ionically interacts with the protonated amino group of cysteine (-$NH3^+$ OOC-), and the thiol/thiolate group of cysteine forms a coordinate or hydrogen-bond interaction with the imidazole nitrogen; or (2) a covalent Michael (thiol-addition) adduct, in which Cys-SH adds across the UCA C=C bond, resulting in a thioether product (S-(3-(4-imidazolyl)-2-carboxypropyl)-cysteine). This reaction eliminates or attenuates vinylic signals and generates new aliphatic resonances. Propose that the cz's-UCA-L-cysteine complex is depicted in Figure 4.2.

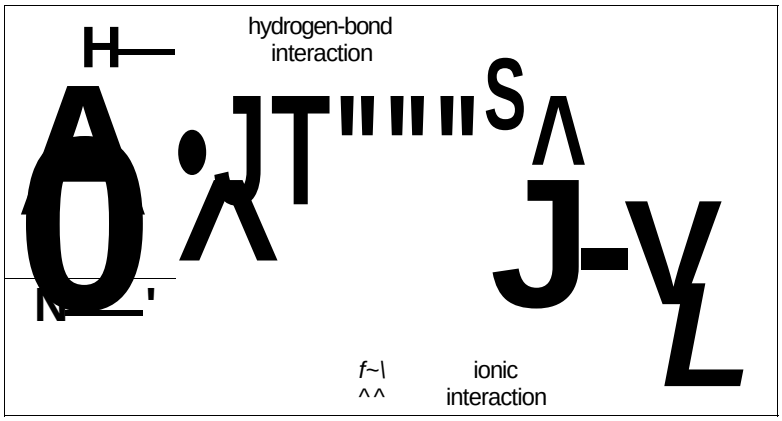

Figure 4.2 Proposed Czs-Urocanic Acid-L-Cysteine Complex was Generated using RCSB.org

Table 4.1
[1]H NMR Chemical Shift Assignments for the Czs-Urocanic Acid-Sodium Sulphide Complex and Czs-Urocanic Acid-L-Cysteine Complex

Spectrum	8 (ppm)	Multiplicity	J (Hz)	Integral	Assignment
1) UCA + Na_2S	8.5	br s			Imidazole H-2
1) UCA + Na_2S	7.12	s			Imidazole H-4
1) UCA + Na_2S	7.45	d	10.5		Vinyl H (cw-CH=)
1) UCA + Na_2S	6.32	d	10.5		Vinyl H (=CH-)
2) UCA + L-Cys	8.48	br s			Imidazole H-2
2) UCA + L-Cys	7.08	s			Imidazole H-4
2) UCA + L-Cys	6.62	d	10.5		Vmyl H (cw-CH=)
2) UCA + L-Cys	6.05	d	10.5		Vinyl H (=CH-)
2) UCA + L-Cys	4.0	t (app)	6.0		L-Cys a-CH
2) UCA + L-Cys	3.12	dd	13.5,5.5		L-Cys P-CH2 (Ha)
2) UCA + L-Cys	2.98	dd	13.5,7.0		L-Cys P-CH2 (Hb)

4.2 Oy-Urocanic Acid-Glutathione Complex

'H-NMR spectral analysis examined the interaction between cz's-urocanic acid and glutathione. The spectrum of free cz's-urocanic acid (Spectrum 1) exhibited characteristic vinyl proton signals in the 8 6.10-6.65 ppm range, along with imidazole proton resonances at 8 7.41 and 8 8.43 ppm, consistent with values reported in the literature. Significant alterations were observed in the spectrum of the reaction mixture with glutathione (spectrum 2). The olefinic resonances were markedly reduced in intensity and shifted downfield/upfield, suggesting the disruption of the conjugated alkene system. New resonances emerged at 8 3.61 ppm (multiplet) and 8 3.09 ppm (multiplet), consistent with a methine proton adjacent to sulphur and a diastereotopic methylene group, respectively. Additional multiplets between 8 2.00 and 3.70 ppm corresponded to glutathione's methylene protons from glutamate, cysteine, and glycine units, while a-proton signals for amino acids appeared in the 8 4.20-4.85 ppm region. The stacked spectra (spectrum 3) highlighted the disappearance or shift of olefinic peaks and the emergence of glutathione-related resonances, indicating successful conjugate formation. The proposed cz's-UCA-glutathione complex is shown in Figure 4.3.

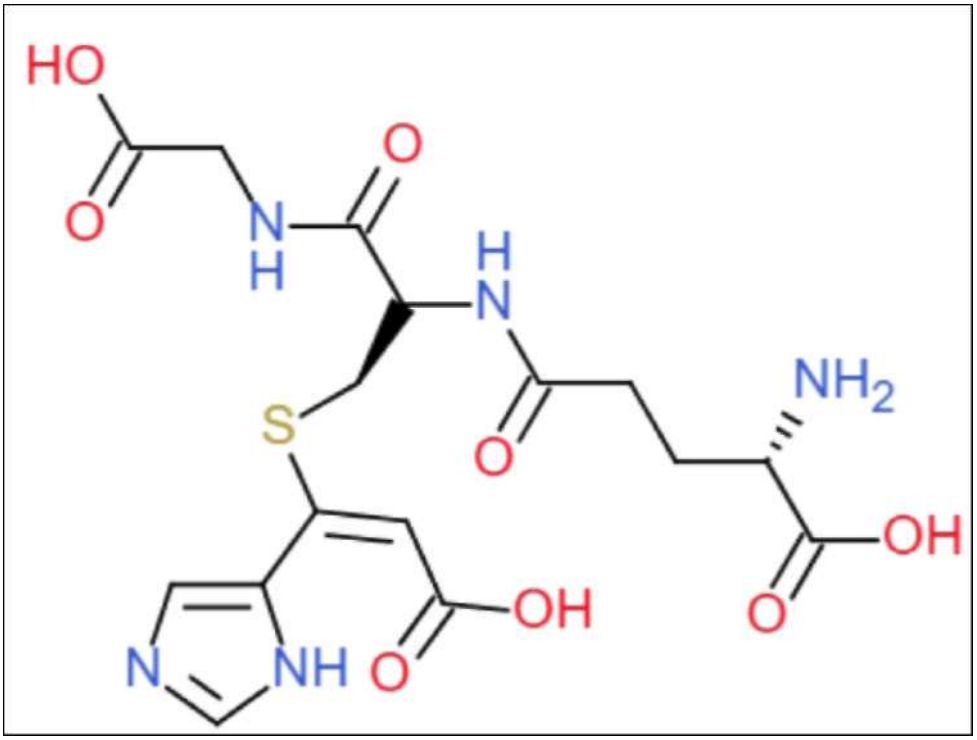

Figure 4.3 Proposed Czs-UCA-Glutathione Complex was Generated using RCSB.org

Table 4.2
'H-NMR Chemical Shift Assignments for the Czs-Urocanic Acid-Glutathione Conjugate.

Chemical Shift (8, ppm)	Multiplicity	Proton Assignment
6.10-6.65	Multiplet	Olefinic protons (cw-urocanic acid)
7.41,8.43	Singlet	Imidazole ring protons
3.61	Multiplet	Methine proton adj acent to sulphur (CH-S)
3.09	Multiplet	Diastereotopic methylene protons next to CH-S
2.00-3.70	Multiplet	Glutamate, cysteine, glycine, and methylene protons
4.20^.85	Multiplet	a-protons of amino acids

4.3 Oy-Urocanic Acid-Sodium Hydrosulfide Complex

The ^-NMR spectrum of the cz's-urocanic acid-sodium hydrosulfide complex revealed that the chemical shift pattern and signal multiplicity suggest preserving the imidazole aromatic core, with minor electronic perturbations attributable to HS coordination. The signal at 8 8.43 ppm corresponded to the downfield-shifted imidazole C2-H (H5) proton, which is deshielded due to its proximity to the nitrogen atoms and

potential hydrogen bonding. The peak at 8 7.79 ppm likely represented the imidazole C4-H (H4), which was slightly shifted relative to the free cz's-urocanic acid, indicating an altered electron density resulting from the HS interaction. The resonance at 8 7.63 ppm is associated with the olefinic proton adjacent to the imidazole ring (H7), with its position reflecting conjugation with the imidazole 7i-system. The large singlet at 8 6.27 ppm was assigned to the olefinic proton adjacent to the carboxyl group (H8), whose upfield nature compared to aromatic protons is consistent with reduced deshielding in the HS -complexed form. The absence of additional peaks for free thiol protons (SH) supported deprotonation to HS and potential nucleophilic addition or coordination at the C7-C8 olefin. Overall, the spectrum supports a stable adduct with minimal proton exchange, retaining the cis geometry while displaying chemical shift changes consistent with electron donation from HS into the conjugated system.

Based on TT-NMR spectra analysis, which showed the persistence of vinylic signals with only minor shifts, the most likely weak adduct between cz's-urocanic acid and HS is a non-covalent, reversible association rather than a genuine C-S bond. Three closely related structural models are consistent with the data in Figure 4.4: (A) an ion-pair/solvated complex in which the carboxylic proton is removed (-COO Na^+) and HS is loosely associated via electrostatic/ion-pairing, with Na^+ acting as a bridge; (B) a hydrogen-bonding complex where HS serves as a hydrogen-bond acceptor to the imidazole N-H and/or the carboxylic OH (if not fully deprotonated), thereby perturbing electronic density but leaving the C=C bond intact; and (C) a nucleophile-7i (charge-transfer) complex in which the sulphide lone pair transiently interacts with the conjugated imidazole-alkene 7i-system, providing reversible, weak stabilization. These scenarios account for the small downfield or upfield shifts observed without losing vinylic resonances.

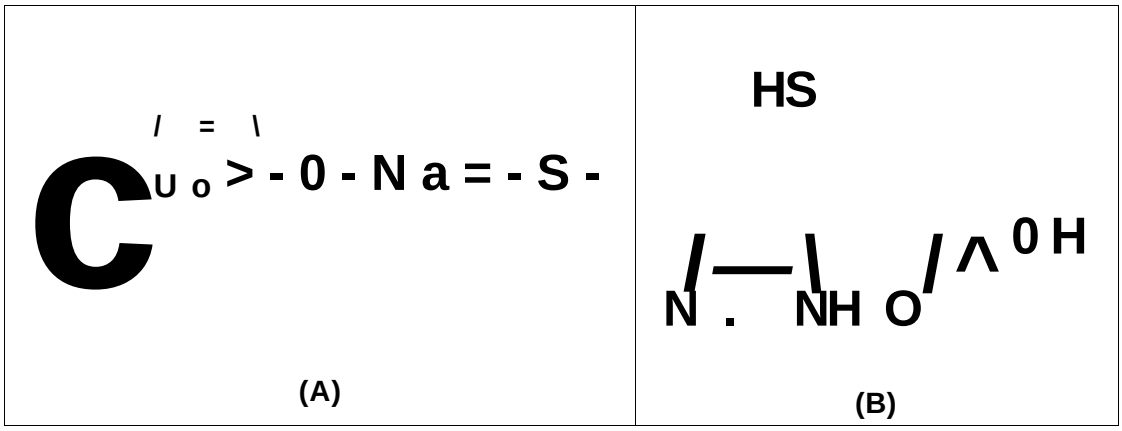

Figure 4.4 Proposed Czs-Urocanic Acid-Sodium Hydrosulfide was Generated using RCSB.org

Table 4.3
^{J}H NMR Chemical Shift Assignments for the Czs-Urocanic Acid-Sodium Hydrosulfide Complex.

5(ppm)	Integration	Multiplicity
-8.43	**1H**	s (or weakly coupled)
-7.79	**1H**	s/d
-7.63	**1H**	d (J -15-16 Hz)
-6.27	**1H**	d (J -15-16 Hz)

Based on these results, the interaction of sodium hydrosulphide (NaHS), a well-known inorganic reactive sulphur donor, with cz's-urocanic acid (czs-UCA), a photoreactive imidazole-containing histidine metabolite, produced a new unreported conjugated compound named 4-imidazoleacrylic-3-thiol, whose chemical structure is shown in Figure 4.4 (B). Although phase 1 demonstrated that *cis-XJCA* can directly react with various sulphide donors non-enzymatically, this interaction does not clarify how the GST is expressed in the pathway. Therefore, a molecular docking study in phase 2 was conducted to examine whether these cz's-UCA-RSS conjugates specifically GS(CIE) if the molecule could interact with GST, providing insight into their potential functional role in cellular redox pathways.

4.4 Binding Affinity of Molecular Docking Analysis

Docking Analysis revealed that the binding affinity of GST with GS(CIE) is higher than the binding affinity of the reference drug, sulforaphane. Comparison value and details of the interaction of GST and the ligand are shown in Table 4.4.

Table 4.4
The Details Binding Affinities Results

Ligand	Affinity (kcal/mol)	Interacting Residues	Type of Interaction
GS(CIE)	**-6.7**	Tyr7, Gln64, ArglOO, Asn204	Hydrogen Bond
		Tyrl08	Pi-Alkyl
Sulforaphane	**-3.6**	Gly205	Hydrogen Bond
		Tyrl08	Pi-Sulphur

Table 6 presents the binding affinity results of GST with GS(CIE) and sulforaphane. The binding affinity of GS(CIE) was measured at -6.7 kcal/mol, whereas GST and sulforaphane exhibited a lower binding affinity of-3.6 kcal/mol. Molecular docking analysis demonstrated that the GS(CIE) shows a strong and stable binding affinity for GST, supported by multiple intermolecular interactions that enhance overall binding stability. Sulforaphane, a recognized GST inhibitor, was docked with GST for reference. The binding affinity of sulforaphane to GST was measured at -3.6 kcal/mol. The binding affinity was observed to be marginally lower in comparison to GS(CIE). The residues interacting at the active site of GST, docked with GS(CIE) and sulforaphane, are presented in Table 6, based on simulation results from Discovery Studio (BIOVIA). However, molecular docking scores indicate predicted binding interactions but do not inherently correlate with actual enzymatic activation or inhibition. Although the docking results suggested favourable interactions between GST and GS(CIE), experimental validation was performed in Phase 3 to determine the biological effects of these interactions. Phase 3 involved an *in vitro* study of HaCaT cells under UVB exposure to assess changes in cell viability.

4.5 Docking Pose Analysis

To assess the polar interaction between the compounds and the residues at the GST binding site, the highest binding pose of GS(CIE) is shown in Figure 4.5. Polar interaction between GST and sulforaphane is shown in Figure 4.6. This interaction was visualised using PyMOL. Therefore, there is an interaction based on the residues between GST and each ligand.

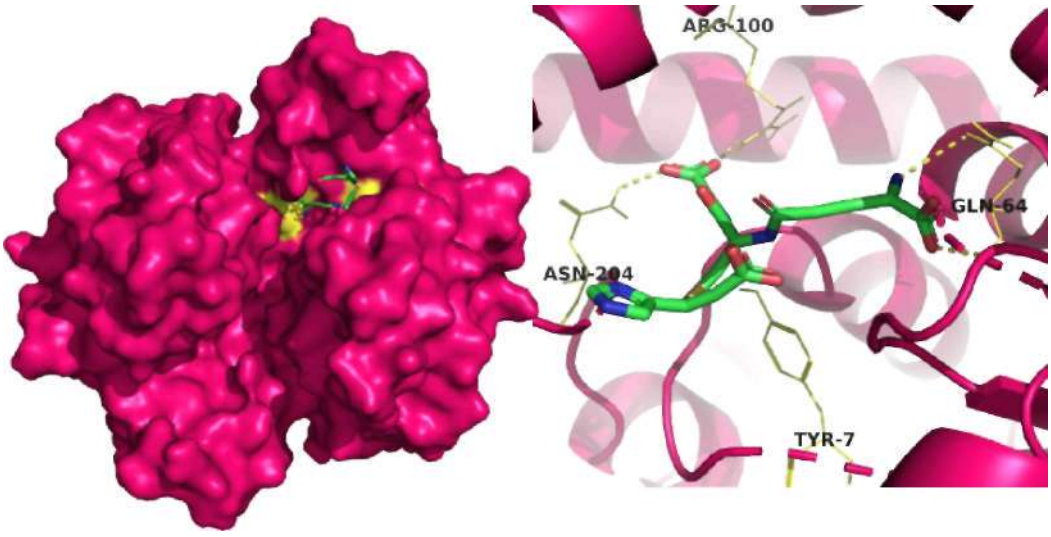

Figure 4.5 3-D Interaction of GST and GS(CIE) at Residues Tyr7, Gln64, Asn204 and ArglOO, Generated by PyMOL

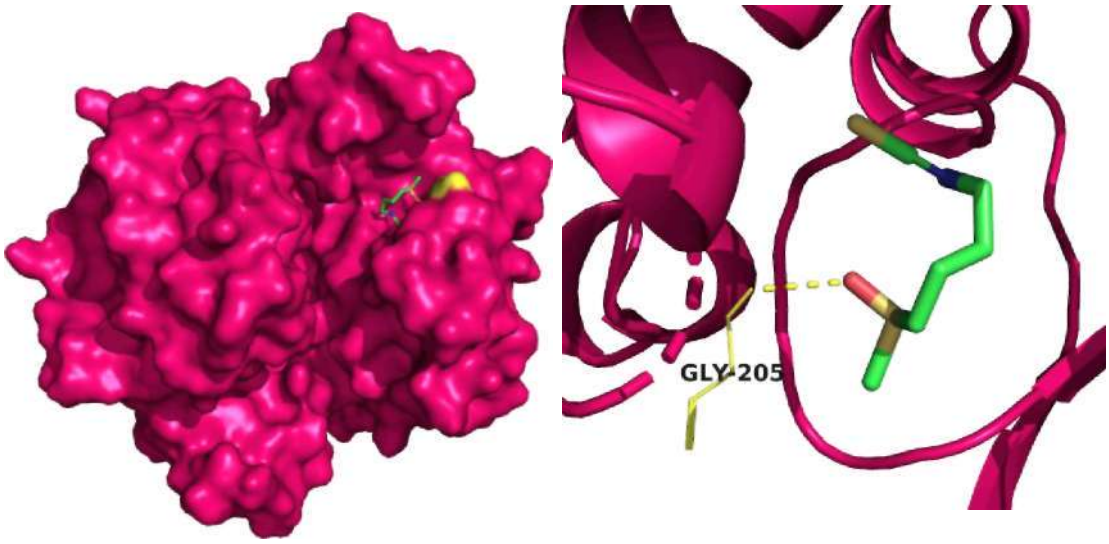

Figure 4.6 3-D Interaction of GST and Sulforaphane at Residue Gly-205, Generated by PyMOL

4.6 Effect of *cis-VCA* and UV Radiation on HaCaT Cell Viability

To determine the cytotoxicity dose of *cis-UCA* for this study, cells were exposed to increasing concentrations of *cis-UCA* (0, 0.1, 0.25, 0.5, and 1 mM) for 24 hours and then evaluated using the MTT assay. As illustrated in Figure 4.7, the cell viability test by MTT assay in HaCaT cells treated with various concentrations of *cis-UCA* for 24 h

(A) and after exposure to UVB (B). Data are represented as the mean ± SEM of three individual replicates; * $p<0.05$ and ** $p<0.01$ compared to the control group.

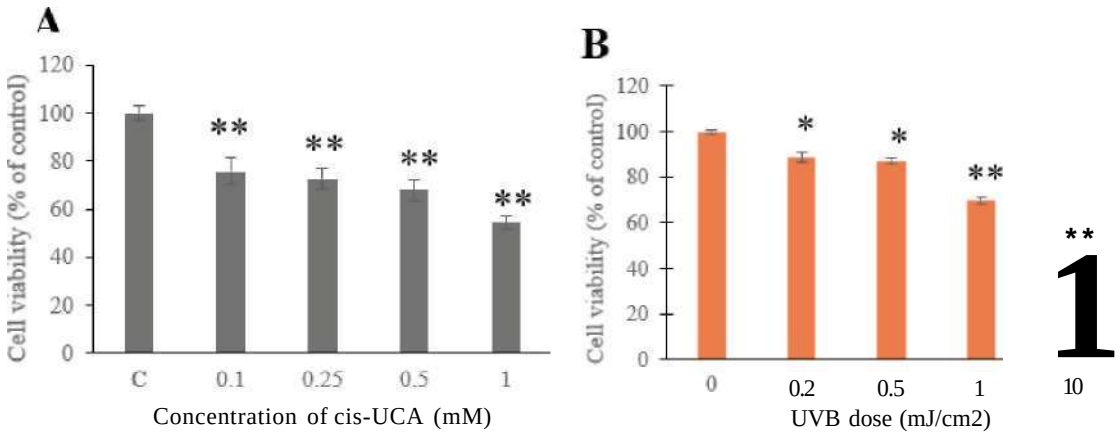

Figure 4.7 Cell Viability Test by MTT Assay in Hacat Cells Treated with Various Concentrations of *Cis-UCA* for 24 H (A) and after Exposure to UVB (B). Data are Represented as the Mean ± SEM of Three Individual Replicates: * $p<0.05$ And ** $p<0.01$ in Comparison to the Control Group.

Figure 4.7(A) illustrates a notable decrease in cell viability to 75±5.67% at a 0.1 mM concentration of *cis-UCA* compared to the control (100±3.25%, $p<0.01$), indicating a gradual, dose-dependent inhibition of HaCaT cell proliferation. A reduction in cell viability to 54.50±2.85% was observed with 1 mM *cis-UCA* compared to the control (100±3.25%, $p<0.01$). Figure 4.7 (B) illustrates that exposure to UVB radiation (0.2-10 mJ/cm^2) resulted in a progressive and statistically significant reduction in viability, with $p < 0.05$ at 0.2 mJ/cm^2 and $p < 0.01$ at >1 mJ/cm^2. At the maximum dosage evaluated (10 mJ/cm^2), cell viability decreased to 57.73±0.04 compared to the control group (100±0.17, $p<0.01$). Thus, a concentration of 1 mM *cis-UCA* was chosen for this study and was subsequently exposed to 10 mJ/cm^2 UVB irradiation.

4.7 Effect of Sulphide Donors on HaCaT Cell Viability

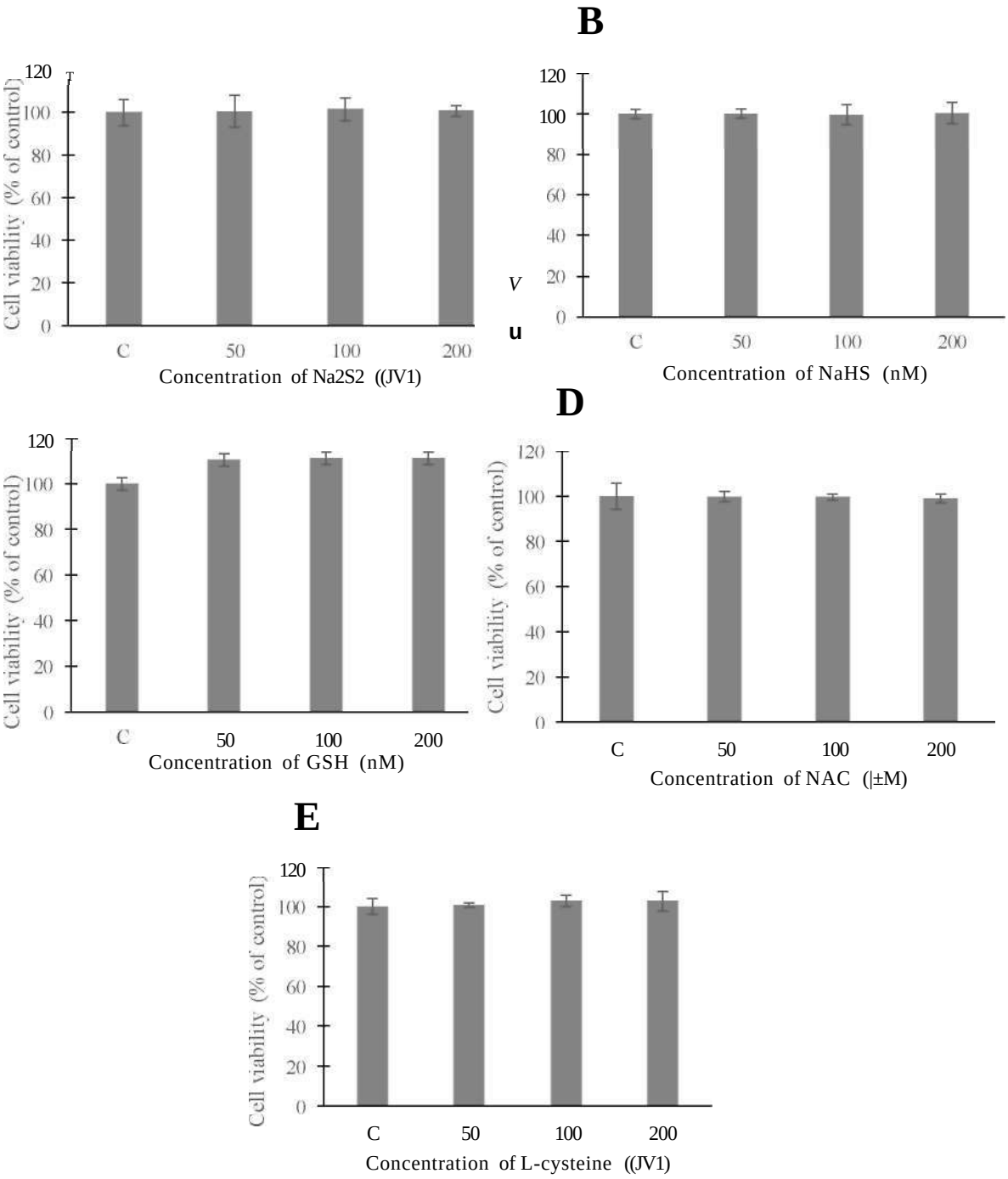

Figure 4.8 Cytotoxicity Profile of Hacat Cells towards Various Concentrations of Na2S2 (A), Nahs (B), GSH (C), NAC (D), And L-Cysteine (E) for 24 H Incubation. Cells without Treatment Served as the Control. Data are Shown as Mean ± SEM. All Experiments were Carried out in Triplicate

The cytotoxicity of sulphide donors, including Na2S2, NaHS, GSH, NAC, and L-cysteine, was investigated in HaCaT cells after 24-hour exposure at concentrations of 50 uM, 100 uM, and 200 uM. Figure 4.8 shows the cytotoxicity profile of HaCaT cells towards various concentrations of Na_2S_2 (A), NaHS (B), GSH (C), NAC (D), and L-cysteine (E) for 24 h incubation. Cells without treatment served as controls.

Data are shown as mean ± SEM. All experiments were carried out in triplicate. The results indicate that cell viability exceeded 90% when treated with RSS, indicating that all five compounds exhibited high biocompatibility compared to the untreated control group across all tested dosages. No statistically significant reductions in viability were observed for any sulphur donors ($p > 0.05$), suggesting that these compounds did not exhibit harmful effects at the tested dose levels.

GSH exhibited a slight trend towards enhanced viability at elevated concentrations compared to the control. The data showed that at 200 uM, GSH enhanced cell viability from 100 ± 4.67% of the control group to 111.30 ± 2.96%. However, this finding was not statistically significant. NaHS and Na_2S2 demonstrated consistent viability across all doses, whereas NAC exhibited a slight decrease in viability to 98.93±1.98% at 200 uM, compared to the control group (100±5.84 %), yet retained values exceeding 90%.

4.8 Effect of *cis-VCA*, Sulphide Donors, and UVB on HaCaT Cell Viability

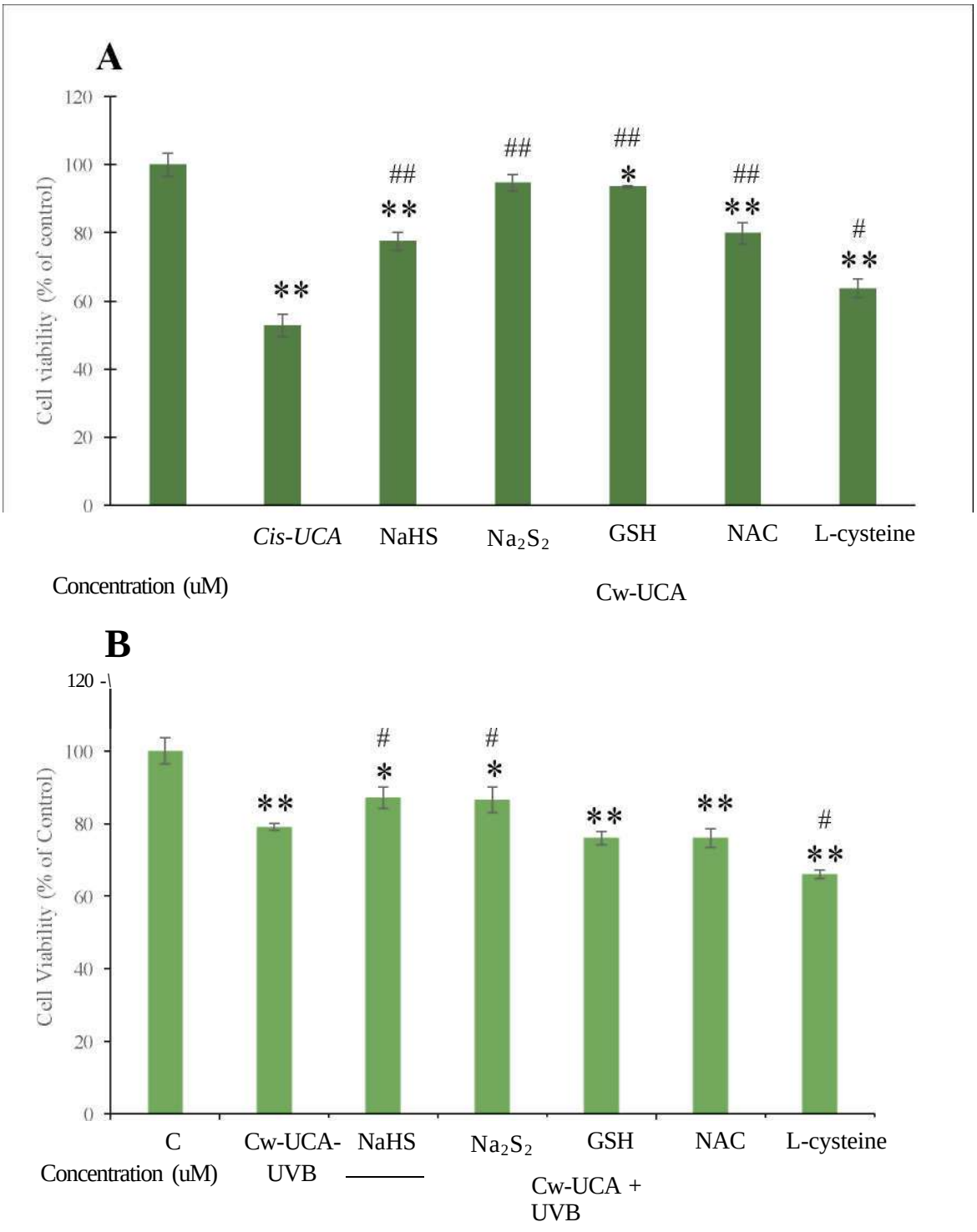

Figure 4.9 Cytotoxicity Profile of Hacat Cells Pretreated with 200 um of Nahs, Na2S2, GSH, NAC, and L-Cysteine towards 1 Mm of *Cis-UCA* (A) and Cells Exposed to UVB (B) for 24 H Incubation. Cells without Treatment Served as the Control. Data are Shown as Mean ± SEM. All Experiments were Carried out in Triplicate; * P<0.05 and ** P<0.01 Compared to the Control Group; # P<0.05 and ## P<0.01 Compared to cw-UCA/cw-UCA + UVB.

Figure 4.9 (A) illustrates that the co-treatment of HaCaT cells with *cis-UCA* (1 mM) and each sulphur compound (200 uM) enhanced cell viability in comparison to treatment with *cis-UCA* alone. UVB exposure significantly reduced cell viability to 52.71± 3.31% compared to the untreated control 100± 3.43% and other cells that were treated with *cis-UCA* and sulphide donours. Exposure to *cis-UCA* alone decreased cell viability to around 55% ($p < 0.01$ compared to control). All treatments involving reactive sulphide species (RSS) significantly enhanced cell viability, with ~80% cells for NaHS (77.45± 2.74%) and NAC (79.8±3.09%), while ~90% cells for both Na_2S_2 (94.67± 2.39%) and GSH (93.48± 0.28%), elevating viability to approximately 80-90% (## $p < 0.01$ vs. *cis-UCA)*, whereas L-cysteine with 63.69± 2.71%, exhibited a moderate rescue effect (~70%) (# $p < 0.05$ vs. cis-UCA).

Figure 4.9 (B) indicates that cells treated with *cis-UCA* and subjected to UVB irradiation demonstrated a notable reduction in cell viability to 79±0.96 compared untreated control (100±3.6, $p < 0.01$), consistent with the synergistic cytotoxic effects resulting from UVB-enhanced stress. Pre-treatment of cells with sulphide donors resulted in a slight reduction of UVB-induced damage; however, this effect was insufficient to fully protect the cells. NaHS (87.07±2.07) and Na_2S_2 (86.49±3.57) exhibited the most significant protective effect (approximately 85%, $p < 0.05$), while GSH (75.99±1.87) and NAC (75.98±2.6) demonstrated moderate rescue (around 75-80%>). L-cysteine with 66.02±1.2 presented the least effect (approximately 65%, $p < 0.05$).

CHAPTER 5
DISCUSSION

This study presents several key findings across the experimental phases. First, *cis-XJCA* was shown to react with sulphide donors readily and undergo non-enzymatic conjugation with a range of reactive sulphur species in a cell-free system, leading to the formation of several identifiable conjugates, including a novel sulphur-containing molecule known as 4-Imidazoleacrylic acid-3-thiol. Second, the *in-silico* study reveals that the molecular docking analysis between GST and cz's-UCA-RSS, specifically the GS(CIE), exhibits a higher binding affinity than the reference drug sulforaphane, which is a known GST agonist. This suggests that the GST is more favourable for binding with GS(CIE), indicating that the GST does not catalyse the formation of GS(CIE), but rather binds with it to recruit more GSH. Next, an *in vitro* assay using UVB-irradiated HaCaT cells shows that while *cis-XJCA* reduces cell viability under UVB stress, the presence of RSS mitigates the cytotoxic effect.

To interpret these findings in greater depth, it is necessary to revisit and compare them with the pathway proposed by Kinuta *et al.* (2001), which forms the basis of the current understanding of the *cis-UC* A metabolism pathway. Kinuta's proposed pathway suggested that the GS(CIE) is converted to Cys (CIE) by removing two amino acids, glutamate and glycine. Nonetheless, this proposed mechanism (highlighted in the red box, Figure 5.1) was not accompanied by any scientific evidence, indicating that the processes involving the conversion of GS(CIE) onwards were based on the scientific knowledge available at that time. No findings on the formation of Cys (CIE)-Gly intermediate were stated in their published works (Kinuta *et al.*, 2001). Additionally, this proposed pathway raises substantial doubts due to several compelling reasons. For instance, conversion of GS(CIE) into Cys (CIE) involves the elimination of two amino acids from the glutathione structure. This conversion process proposed by Kinuta *et al* (2001) requires substantial energy and may necessitate a different catalytic system, such as enzymes.

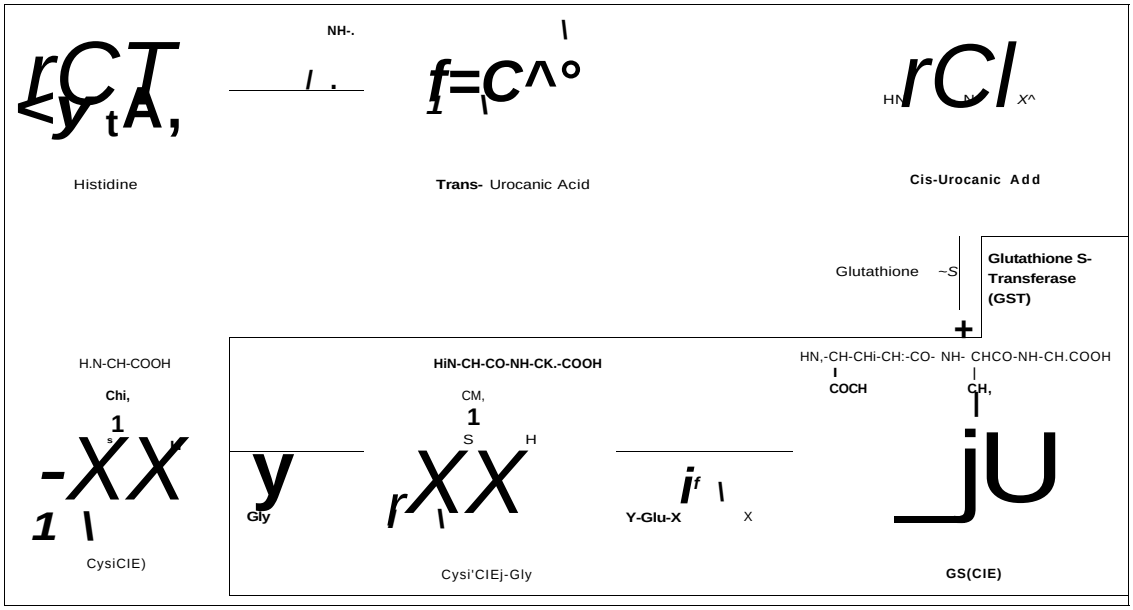

Figure 5.1 C/5-UCA Metabolism Pathway by Kinuta et al. (2001) was Generated using RCSB.Org. The Red Box Highlights the Missing Gap in this Proposed Mechanism

A different perspective on *cis-UCA* biochemical properties needs to be re-evaluated to explain the missing pieces in Kinuta's *cis-UCA* metabolism framework. Given that the energy absorbed from UV irradiation affects the UCA's *trans*- and cis forms, it is thought that the energy transfer may excite the molecule to some extent. With this thought, it is believed that *cis-UCA* theoretically exists in a higher energy state, rendering it highly reactive. Nucleophiles, for example, supersulphides, are known for their robust electron-donating capacity and easily attack electron-deficient centres in electrophiles. Indeed, in this study, we observed that the *cis-UCA* can readily react with glutathione, one of the RSS, through nucleophilic attack, forming GS(CIE), without the involvement of GST. Again, using the same concept, we experimented with the *cis-UCA* in combination with other RSS donors, including L-cysteine, NaHS, and Na2S2, in a cell-free system. This aligns with our hypothesis, where *cis-UCA* can directly react with RSS and form a conjugate without the involvement of GST

In addition, ^{1}H-NMR analysis supported that *cis-UCA* can interact with multiple RSS, including NaHS, Na2S2, L-cysteine, and GSH, without the need for enzymatic catalysis by GST. The cz's-UCA-glutathione spectra revealed an apparent loss of vinylic signals and the emergence of new methine and methylene peaks, indicating covalent

thioether synthesis via Michael addition. L-cysteine's a- and P-protons exhibited similar perturbations while keeping the vinyl peaks, suggesting a combination of non-covalent ionic interactions and partial covalent addition. In contrast, NaHS and Na2S2 retained the olefinic resonances with modest alterations, indicating reversible ionic or hydrogen-bond-assisted associations rather than permanent C-S bond formation.

Interestingly, based on the NMR results of *cis-UCA* incubation with NaHS, the reaction produces a novel compound, 4-imidazoleacrylic acid-3-thiol (Figure 13B). Therefore, this could provide justification for the proposed alternative pathways for *cis-UCA* that incorporate the newly identified conjugation reactions. This result not only confirms the successful chemical coupling of a sulfur-based moiety with *cis-UCA* under the tested conditions, but it also introduces a novel compound that has not been previously described in the literature, thereby expanding our understanding of *cis-*UCA's chemical reactivity and potential biochemical transformation pathways. In addition, this identification of a novel compound provides the first evidence that *cis-UCA* can undergo direct-thiol-based modification in the absence of enzymatic activity. This discovery reveals an alternative redox-related metabolic route. However, the inability of this compound to be identified in the *in vitro* model led us to think that the *cis-UCA* can easily react with thiol-containing compounds, both low-molecular-weight compounds such as GSH and CysSH, and potentially respond with high-molecular-weight components, such as proteins.

The results of this study indicate that the conjugation of *cis-UCA* with RSS can occur effectively in the absence of enzyme catalysis. For L-cysteine and GSH, the conjugates obtained matched those reported by Kinuta *etal.* (2001); however, based on the Phase 1 results, they were formed without the involvement of GST. This indicates that enzyme-independent thiol conjugation can occur directly, while GST may instead play a regulatory or stabilizing role, consistent with the known multifunctional behavior of GST enzyme (Hayes & Pulford, 1995; Tew, 2007). This suggests that the reaction is non-enzymatic, in contrast to earlier studies that highlighted the role of GST, which is typically abundantly expressed in keratinocytes (Kinuta *etal,* 2003). This contradiction prompts a mechanistic inquiry: if GST is unnecessary for conjugation, what is the enzyme's function within the overall pathway? So, we hypothesized that GST may not

catalyze the conjugation but rather interacts with the glutathione-cz's-UCA conjugate post-formation.

Molecular docking study corroborates this hypothesis, indicating that the binding affinity of GST for the glutathione conjugate is markedly superior to that for *cis-XJCA* itself. The binding affinity was notably higher than that recorded for sulforaphane, a recognized GST inhibitor utilized as a reference ligand (Prasetyawan *et al,* 2025). The data indicate that the glutathione conjugate may function as a regulator of GST activity, therefore affecting subsequent antioxidant responses. Initially, docking studies were performed between the GST-only and cz's-UCA-only settings, but the results showed no significant binding affinity. As a result, further docking was conducted between GST and the GS(CIE), which exhibited higher binding affinity. In these *in silico* studies, sulforaphane was used as a reference ligand due to its known affinity for GST, particularly the GSTP1 isoform (Licznerska, Szaefer, & Krajka-Kuzniak, 2021). Sulforaphane, a naturally occurring isothiocyanate derived from cruciferous vegetables such as broccoli, has been widely recognised for inhibiting GSTs. Its inhibitory action is primarily mediated through the covalent modification of cysteine residues at the active site of GST, leading to reduced enzymatic activity (Dinkova-Kostova *etal.,* 2008). With these characteristics, sulforaphane was employed as a reference compound to benchmark the binding affinity and interaction profile of the GS(CIE) with GST.

The binding affinities determined the interaction of the protein and ligand. This *in-silico* activity demonstrates that GS(CIE) has a stronger binding affinity than sulforaphane. The docking poses show that the protein and ligand interact using various types of bonds. Hydrogen bonds were visualised through PyMol (Schrodinger, LLC, 2015), and other bonds were observed through Discovery Studio (BIOVIA). Based on the visualisation, GS(CIE) formed two hydrogen bonds with Gln64 at this site. Residues Tyr7, Gln64, ArglOO, Asn204, and Tyrl08 significantly contributed to the binding with GS(CIE), resulting in a binding affinity of the complex calculated to be -6.7 kcal/mol. For sulforaphane, the Gly205 residue of GST formed a hydrogen bond, and the Tyrl08 residue interacted with sulforaphane, forming a pi-sulphur bond. The binding affinity was calculated to be -3.6 kcal/mol.

This poses a "chicken-and-egg" dilemma: does GST facilitate the initial creation of the conjugate, as suggested by Kinuta *et al* (2001), or does the conjugate form autonomously and later engage with GST to augment its activity? Our findings support the latter idea, suggesting that *cis-XJCA* and GSH can easily form a conjugate independently of enzymatic intervention, which subsequently facilitates GST activation. Through this method, GST may facilitate the recruitment of more GSH molecules and enhance cellular antioxidant defences. The proposed pathway is shown in Figure 5.2 below

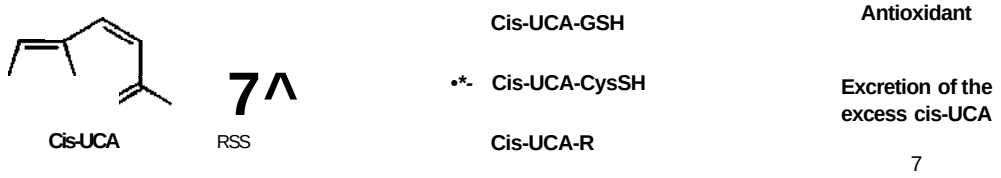

Figure 5.2 Proposed Pathway of *Cis-UCA* Metabolism that was Generated by Biorender

For this proposed pathway, in the first line, the *cis-UCA* can directly react with RSS, specifically glutathione (GSH), and form a GS(CIE), where the conjugate compound activates or binds with GST to recruit more GSH for antioxidant purposes. The second line in this proposed pathway, *cis-UCA*, can directly react with a molecule containing cysteine and form a Cys (CIE), a polar form of the molecule that facilitates the excretion of excess *cis-UCA*. The final step in the proposed pathway involves *cis-UCA* reacting with any biological molecule containing thiols (SH), including proteins. However, further study is needed to elucidate this mechanism, as its biological function remains unknown.

These results signify a significant finding where *cis-UCA* is not just a simple chromophore but may play a significant role as a phototransmitter. Further investigations are required for validation. In addition, the same experiment was repeated using the *trans-UCA* and RSS donors, and no conjugation was observed. Hence, the structural changes observed between the *trans-UCA* and *cis-UCA* (Figure 1) indicate the "unlocking" mechanism. The shifted position of the carbonic acid group at carbon 5 in the UCA allows this compound to be structurally more "open" and readily dock

with other compounds, particularly the nucleophile. These findings also suggest that *cis*-UCA can be neutralised via irreversible covalent conjugation and reversible complexation, depending on the RSS implicated. This study challenges the canonical Kinuta *et al* (2001) mechanism, which is based on GST-mediated glutathione conjugation, and proposes an alternative GST-independent detoxification approach. This chemical evidence directly supports the Phase 2 molecular docking results, which showed that *cis*-UCA had a low binding affinity for GST. However, the *cis*-UCA-GSH conjugate had a higher affinity, implying that GST may preferentially recognise and process pre-formed conjugates rather than catalyse their initial formation.

The physiological significance of this process is substantiated by the photochemical framework of *cis*-UCA production. *Cis*-UCA is produced from *trans*-UCA through UVB irradiation of the skin (McLoone *et al*., 2005), a condition associated with increased levels of ROS (Norval, 2001). The capacity of *cis*-UCA to create conjugates with thiol-containing compounds may thus signify a defensive mechanism against oxidative stress. *Cis*-UCA may be regarded as a prospective phototransmitter molecule, connecting UV exposure to redox-regulated biological responses. Additional investigation is necessary to examine this potential, especially through the testing of *cis*-UCA in phototransmission models. Furthermore, our data indicate that sulphur donors, including NaHS and GSH, interact with *cis*-UCA in a way that is independent of GST. This suggests that additional thiol-containing compounds, such as protein-bound thiols, may also participate in conjugation with *cis*-UCA. These interactions may expand the range of *cis*-UCA reactivity in cellular contexts, offering new insights into its dual function in both phototoxic and protective mechanisms.

Furthermore, the results suggest that GS(CIE) exhibits a higher binding affinity than sulforaphane, indicating that the glutathione conjugate may interact more effectively with GST in biological systems, potentially enhancing its role in detoxification and cellular protection. This means, GS(CIE), not GSH, modulates GST activity, potentially playing a crucial role in cellular protection against oxidative stress or UV-induced damage. These interactions were observed in a computational context, raising questions about the potential influence of such conjugation on biological outcomes in living cells. Based on these *in silico* findings, it was essential to assess

whether these conjugation events affect the cellular response to *cis-UCA* under physiological stress conditions.

This insight is further supported by our *in vitro* HaCaT data. The *in vitro* MTT assay assessed the physiological effects of czs-UCA-RSS interactome in HaCaT cells exposed to UVB irradiation. The results showed almost a 50% reduction in cell viability for the *cis-UCA* treatment group compared to the czs-UCA-RSS exposed to UVB, indicating a protective effect against UVB-induced damage. In alignment with previous findings, treatment with *cis-UCA* alone resulted in a moderate decrease in cell viability compared to the untreated control, suggesting that the tested concentration possesses inherent cytotoxic effects. Recent findings suggest that *cis-UCA*, particularly under UV exposure, may contribute to immunosuppression or cellular stress by generating reactive intermediates (Bruhs *etal*, 2020). UVB exposure enhanced the cytotoxicity of *cis-UCA*, suggesting that UVB likely increases the reactivity of *cis-UCA*, potentially through enhanced ROS production or tautomeric conversion. The data indicate that *cis-UCA* exerts lethal effects on keratinocytes irrespective of UV radiation, aligning with earlier findings that it can modulate immunological responses and induce oxidative stress in skin cells.

The cytotoxicity of sulphide donors, including NaHS, Na2S2, GSH, NAC, and L-Cysteine, was assessed to evaluate the safety of RSS as therapeutic modulators under *cis-UCA* and UVB stress. All compounds exhibited no significant reduction in cell viability, demonstrating excellent biocompatibility at the tested dose levels, with no notable toxicity observed at concentrations up to 200uM. The findings suggest their potential application as protective agents in contexts of oxidative or electrophilic stress. Co-incubation of *cis-UCA* with each sulphide donor resulted in a notable enhancement in cell viability, with Na2S2 and GSH demonstrating the most significant effects, which is approximately above 90% compared to the *cis-UCA* alone. The findings corroborate the hypothesis that sulphur-containing compounds can directly conjugate with *cis-UCA* or its electrophilic intermediates, thereby supporting a non-enzymatic sulphur conjugation pathway where it neutralizes its cytotoxic potential, reduces *cis-UCA* toxicity, and enhances the UV-induced antioxidant response. The effect was similarly noted under UVB-enhanced stress conditions, albeit with a slight reduction in the degree

of protection. The presence of sulphur donors notably improved cell viability, underscoring their therapeutic potential in UVB-damaged skin environments.

The findings in this study carry important pathological implications. As reported, the accumulation of *cis-UCA* following exposure to UV contributes to immunosuppression by impairing Langerhans cell function and triggering the oxidative stress pathway, which is known to facilitate the early stages of photocarcinogenesis. Again, in this study, Phase 1 demonstrated that cis-UCA can directly react with RSS to form a conjugate, suggesting that alternative metabolic routes may influence UV-related skin conditions. For example, the formation of the *cis-UCA* conjugate compound and its compatibility in binding with GST may alter the redox buffering capacity in keratinocytes, potentially modulating responses or susceptibility to UV-driven DNA damage. Given that dysregulated redox signalling and impaired detoxification pathways are hallmark contributors to conditions such as squamous cell carcinoma, basal cell carcinoma, and chronic inflammatory skin diseases, these newly identified czs-UCA-RSS interactions may represent previously unrecognised biochemical events that modify disease risk or progression. Although further in vivo studies are required, the present findings introduce a mechanistic link between altered *cis-UCA* metabolism and pathological skin outcomes described in earlier literature.

In addition, the current findings indicate that further extensive and systematic investigations are required to better understand the underlying molecular mechanisms of *cis-UCA. A* better understanding of these pathways will not only elucidate the compounds' direct biochemical interactions. However, it will also help the researcher to comprehend how *cis-UCA* regulates, modulates, and potentially restores the physiological properties of the skin in both standard and stress-induced settings. This mechanistic understanding is critical for closing the gap between basic experimental research and clinical applications in dermatology and pharmacology. In particular, the current study provides persuasive evidence that the interaction of NaHS, a proven inorganic RSS donor, with *cis-UCA* creates a previously unknown conjugated molecule. This novel product demonstrates *cis-UCAs* chemical plasticity and shows that its reactivity with sulphur-based donors could be a feasible and underexplored avenue for altering its biological function. The discovery of such a molecule, which has

not been previously reported in the literature, represents a significant advance in our understanding of *cis*-UCA chemistry and opens new avenues for therapeutic applications.

Despite the need for additional mechanistic studies, such as structural characterization, kinetic profiling, and pathway mapping, this discovery represents a significant step forward in advancing our study to more clinically relevant scenarios. By broadening the scope to include other RSS with improved clinical compatibility, bioavailability, and safety profiles, it may be possible to develop synergistic treatment strategies that amplify the beneficial effects of *cis*-UCA while also introducing additional therapeutic benefits such as antioxidant reinforcement, anti-inflammatory modulation, and photoprotection. Such an approach may ultimately lead to the development of novel skin-protective agents or adjuvant therapies, thereby accelerating the translation of laboratory findings into practical interventions for skin health and disease prevention.

In conclusion, the discovery that *cis*-UCA can form new conjugates with RSS donors, such as NaHS, supports the chemical feasibility of these reactions in a controlled environment and provides a framework for investigating a broader class of sulfur-containing bioactive molecules. By combining chemical synthesis, mechanistic biochemistry, and therapeutic design, this integrated strategy holds great promise for advancing the field toward tailored, evidence-based dermatological treatments that meet both preventive and therapeutic needs.

CHAPTER 6
CONCLUSION AND RECOMMENDATIONS

This research studied the mechanistic function of RSS conjugation in influencing the biological effects of *cis-UCA* when exposed to UVB irradiation in HaCaT keratinocytes. This study examined deficiencies in the *cis-UCA* metabolic pathway, as outlined by Kinuta *et al* (2001), with a specific focus on the unclear transition from GS(CIE) to Cys(CIE). In a GST-independent cell-free system, *cis-UCA* readily formed conjugates with various sulphide donors, including GSH, L-cysteine, NaHS, and Na2S2. This suggests that conjugate formation may occur spontaneously without needing enzymatic catalysis, highlighting the possibility of non-enzymatic detoxification pathways *in vivo.* Molecular docking analysis indicated that the GS(CIE) exhibited a greater binding affinity for GST than sulforaphane, a recognised GST modulator. This suggests that, although *cis-UCA* exhibits low affinity for GST, GS(CIE) may serve as a substrate or ligand for GST-mediated transport or following biotransformation, thereby establishing a potential mechanistic connection to downstream metabolism.

In vitro cytotoxicity assays conducted on HaCaT cells indicated that *cis-UCA* induces cell death in a dose-dependent manner, with effects increased by UVB irradiation. Pre-treatment with sulphide donors significantly improved cell viability under UVB-exposed and non-exposed conditions, strengthening the hypothesis that sulphide conjugation alleviates cz's-UCA-induced cytotoxicity. The observed protective effect aligns with the hypothesized function of RSS conjugation in minimizing the availability of free, bioactive *cis-UCA.* These findings collectively support a mechanistic model in which RSS donors conjugate with *cis-UCA* through a non-enzymatic pathway, potentially followed by GST-mediated processing, resulting in fewer toxic metabolites. This conjugation pathway may signify a previously overlooked regulatory checkpoint in the biochemical response of skin to UVB irradiation.

Despite these findings, a few limitations should be acknowledged. NMR was used to confirm conjugate structures in a cell-free environment, but this was not verified

in cellular contexts, and no in-cell metabolomic profiling was performed. Without biochemical or kinetic validation, GST-ligand interactions were investigated solely by computational docking. Although the UV exposure was measured using a UV irradiance photometer to measure the UVB exposure data, the timing of the UV exposure was measured using a timer, which may have introduced uncertainty in the dose estimation. Furthermore, all cellular investigations were primarily conducted on HaCaT keratinocytes, which limits the extrapolation to other skin cell types. The work was entirely *in vitro*, with no *in vivo* or *ex vivo* validation.

To overcome these shortcomings, future studies should incorporate targeted metabolomic analysis in cellular systems to demonstrate the intracellular production and stability of *cis*-UCA-RSS conjugates, as well as GST enzymatic assays to validate docking predictions. Furthermore, LC-MS and HPLC can be used to quantify 4-imidazoleacrylic acid-3-thiol and measure oxidative stress markers. The experimental scope should be expanded to include more skin-relevant cell types and co-culture models. Finally, validation in *in vivo* or reconstructed human skin models will be required to determine whether the protective role of RSS conjugation observed *in vitro* translates to physiologically relevant conditions and whether the protective concentrations of RSS donors are feasible in living systems.

In short, our investigation verifies the conjugation ability of *cis*-UCA with RSS and underscores its potential as a chemical defence mechanism against oxidative and electrophilic stress in the skin. This discovery may facilitate a novel research trajectory that utilizes *cis*-UCA-RSS conjugation to prevent and treat several developing cutaneous disorders, such as photoaging, inflammatory dermatoses, and potentially skin malignancies associated with redox dysregulation. Comprehensive mechanistic studies and *in vivo* research will be crucial to thoroughly clarify the biological significance and therapeutic potential of this relationship.

REFERENCES

Abbas, K., Qadir, M. I., & Anwar, S. (2019). The role of melanin in skin cancer. *Critical Reviews™ in Eukaryotic Gene Expression,* 29(1).

Akaike, T., Ida, T., Wei, F. Y., Nishida, M., Kumagai, Y., Alam, M. M., ... & Motohashi, H. (2017). Cysteinyl-tRNA synthetase governs cysteine polysulfidation and mitochondrial bioenergetics. *Nature communications,* 5(1), 1177.

Ali Musa, A. Y., Abdul Hamid, H, & Husain, N. (2025). Ying and yang of urocanic acid in skin pathogenesis: a mini review on its metabolism and effects. *International Journal of Pharmaceutical, Nutraceutical and Cosmetic Science (IJPNaCS),* 5(1), 71-81.

Anastassakis, K. (2022). Sulfur (S). In *Androgenetic Alopecia From A to Z: Vol 2 Drugs, Herbs, Nutrition and Supplements* (pp. 357-362). Cham: Springer International Publishing.

Ansary, T. M., Hossain, M. R., Kamiya, K., Komine, M., & Ohtsuki, M. (2021). Inflammatory molecules associated with ultraviolet radiation-mediated skin aging. *International Journal of Molecular Sciences,* 22(8), 3974.

Arentsen, H. C, Jansen, C. F., Hulsbergen-Van de Kaa, C. A., Laihia, J. K., Pylkkanen, L., Leino, L., ... & Witjes, J. A. (2012). Antitumor effects of cz's-urocanic acid on experimental urothelial cell carcinoma of the bladder. *The Journal of urology,* 757(4), 1445-1449.

Baker, P., Huang, C, Radi, R., Moll, S. B., Jules, E., & Arbiser, J. L. (2023). Skin barrier function: the interplay of physical, chemical, and immunologic properties. *Cells,* 72(23), 2745.

Barresi, C, Stremnitzer, C, Mlitz, V., Kezic, S., Kammeyer, A., Ghannadan, M., ... & Eckhart, L. (2011). Increased sensitivity of histidinemic mice to UVB radiation suggests a crucial role of endogenous urocanic acid in photoprotection. *Journal of investigative dermatology,* 737(1), 188-194.

Barayeu, U., Sawa, T., Nishida, M., Wei, F. Y., Motohashi, H, & Akaike, T. (2023). Supersulfide biology and translational medicine for disease control. *British Journal of Pharmacology.*

Baumann, L., Bernstein, E. F., Weiss, A. S., Bates, D., Humphrey, S., Silberberg, M., & Daniels, R. (2021, September). Clinical relevance of elastin in the structure and function of skin. *In Aesthetic surgery journal open forum* (Vol. 3, No. 3, p. ojab019). US: Oxford University Press.

Bertino, L., Guarneri, F., Cannavo, S. P., Casciaro, M., Pioggia, G., & Gangemi, S. (2020). Oxidative stress and atopic dermatitis. *Antioxidants*, 9(3), 196.

Biovia, D. S. (2017). Discovery studio visualizer. *San Diego, CA, USA, 936,* 240-249.

Bilska-Wilkosz, A., & Iciek, M. (2022). Reactive Sulfur Species (RSS) in physiological and pathological conditions and in therapy. *Antioxidants*, 77(8), 1576.

Bolton, S. G., & Pluth, M. D. (2020). Modified cyclodextrins solubilize elemental sulfur in water and enable biological sulfane sulfur delivery. *Chemical Science*, 77(43), 11777-11784. https://doi.org/10.1039/d0sc04137h

Bothwell, J. H., & Griffin, J. L. (2011). An introduction to biological nuclear magnetic resonance spectroscopy. *Biological Reviews, 86(2),* 493-510.

Brem, R., Guven, M., & Karran, P. (2017). Oxidatively-generated damage to DNA and proteins mediated by photosensitized UVA. *Free Radical Biology and Medicine, 107,* 101-109.

Bromfield, G., Dale, D., & De, P. (2015). Canadian Cancer Society, s Advisory Committee on Cancer Statistics. *Canadian cancer statistics, 2015.*

Bruhs, A., Eckhart, L., Tschachler, E., Schwarz, T., & Schwarz, A. (2016). Urocanic acid: an endogenous regulator of Langerhans cells. *Journal of Investigative Dermatology*, 736(8), 1735-1737.

Chen, Q., Wei, N., & Lu, Y. (2024). A modified protocol for studying filaggrin degradation using a reconstructed human epidermis model under low and high humidity. *International Journal of Cosmetic Science, 46(3),* 380-390.

Choi, E. H., & Kang, H. (2023). Importance of stratum corneum acidification to restore skin barrier function in eczematous diseases. *Annals of dermatology, 36(1),* 1.

Damian, D. L., Barnetson, R. S. C, & Halliday, G M. (1999). Low-dose UVA andUVB have different time courses for suppression of contact hypersensitivity to a recall antigen in humans. *Journal of investigative dermatology, 112(6).*

Damian, D. L., Halliday, G. M., & Barnetson, R. S. C. (1997). Broad-spectrum sunscreens provide greater protection against ultraviolet-radiation-induced suppression of contact hypersensitivity to a recall antigen in humans. *Journal of investigative dermatology, 109(2),* 146-151.

Decara, J. M., Aguilera, J., Abdala, R, Sanchez, P., Figueroa, F. L., & Herrera, E. (2008). Screening of urocanic acid isomers in human basal and squamous cell carcinoma tumors compared with tumor periphery and healthy skin. *Experimental dermatology,* 77(10), 806-812.

De Fabo, E. C, & Noonan, F. P. (2002). Human health and Arctic ozone depletion. In *UV Radiation and Arctic Ecosystems* (pp. 307-315). Berlin, Heidelberg: Springer Berlin Heidelberg.

Denisow-Pietrzyk, M. (2021). Human skin reflects air pollution-a review of the mechanisms and clinical manifestations of environment-derived skin pathologies. *Polish Journal of Environmental Studies, 30(4),* 3433-3444.

Denizalti, M., & Durlu-Kandilci, N. T. (2024). Hydrogen sulfide (H2S) and reactive oxygen species (ROS) scavengers have a protective effect on carbachol-induced contractions that are impaired by high glucose in detrusor smooth muscle. *Journal of Urological Surgery.*

Dinkova-Kostova, A. T. (2008). The effectiveness of the isothiocyanate sulforaphane in chemoprotection. In *V International Symposium on Brassicas and XVI International Crucifer Genetics Workshop, Brassica 2008 867* (pp. 27-36).

Dobrica, E. C, Cozma, M. A., Gaman, M. A., Voiculescu, V. M., & Gaman, A. M. (2022). The involvement of oxidative stress in psoriasis: a systematic review. *Antioxidants, 11(2),* 282.

Dong, K. K., Damaghi, N., Picart, S. D., Markova, N. G., Obayashi, K., Okano, Y., ... & Yarosh, D. B. (2008). UV-induced DNA damage initiates release of MMP-1 in human skin. *Experimental dermatology,* 77(12), 1037-1044.

D'Orazio, J., Jarrett, S., Amaro-Ortiz, A., & Scott, T. (2013). UV radiation and the skin. *International journal of molecular sciences, 14(6),* 12222-12248.

Egawa, M., Nomura, I, & Iwaki, H. (2010). The evaluation of the amount of *cis-and trans-*urocanic acid in the stratum corneum by Raman spectroscopy. *Photochemical & photobiological sciences, 9(5),* 730-733.

Emwas, A. H. M. (2015). The strengths and weaknesses of NMR spectroscopy and mass spectrometry with particular focus on metabolomics research. *InMetabonomics: Methods and protocols* (pp. 161-193). New York, NY: Springer New York.

Emwas, A. H, Szczepski, K., Poulson, B. G, Chandra, K., McKay, R. T., Dhahri, M., ... & Jaremko, M. (2020). NMR as a "gold standard" method in drug design and discovery. *Molecules,* 25(20), 4597.

Feng, C, Chen, X., Yin, X., Jiang, Y., & Zhao, C. (2024). Matrix metalloproteinases on skin photoaging. *Journal of Cosmetic Dermatology, 23(12),* 38Garssen, Vandebriel, Gruijl, D., Wolvers, Dijk, V., Fluitman, & Loveren, V. (1999). UVB exposure-induced

systemic modulation of Thl-and Th2-mediated immune responses. *Immunology, 97(3),* 506-514.47-3862.

Finlayson, L., Barnard, I. R., McMillan, L., Ibbotson, S. H., Brown, C. T. A., Eadie, E., & Wood, K. (2022). Depth penetration of light into skin as a function of wavelength from 200 to 1000 nm. *Photochemistry andPhotobiology,* 95(4), 974-981.

Francioso, A., Baseggio Conrado, A., Mosca, L., & Fontana, M. (2020). Chemistry and biochemistry of sulfur natural compounds: key intermediates of metabolism and redox biology. *Oxidative Medicine and Cellular Longevity, 2020(1),* 8294158.

Frazier, W., & Bhardwaj, N. (2020). Atopic dermatitis: diagnosis and treatment. *American family physician, 101(10),* 590-598.

Gallagher, R. P., Lee, T. K., Bajdik, C. D., & Borugian, M. (2010). Ultraviolet radiation. *Health Promotion and Chronic Disease Prevention in Canada, 29.*

Gilmour, J. W., Vestey, J. P., & Norval, M. (1993). The effect of UV therapy on immune function in patients with psoriasis. *British Journal of Dermatology, 129(1),* 28-38.

Gibbs, N. K., & Norval, M. (2011). Urocanic acid in the skin: a mixed blessing?. *Journal of Investigative Dermatology, 131(1),* 14-17.

Gibbs, N. K., Tye, J., & Norval, M. (2008). Recent advances in urocanic acid photochemistry, photobiology and photoimmunology. *Photochemical & photobiological sciences,* 7(6), 655-667.

Gordon, J. R., & Brieva, J. C. (2012). Unilateral dermatoheliosis. *New England Journal of Medicine, 366(16),* e25.

Gopal, M. (2014). Role of cytokines in tumor immunity and immune tolerance to cancer. *Cancer Immunology: A TranslationalMedicine Context,* 93-119.

Gromkowska-K^pka, K. J., Puscion-Jakubik, A., Markiewicz-Zukowska, R., & Socha, K. (2021). The impact of ultraviolet radiation on skin photoaging—review of in vitro studies. *Journal of cosmetic dermatology,* 20(11), 3427-3431.

Hamid, H. A., Takata, T., Matsunaga, T., & Akaike, T. (2023). A persulfide shield: an endogenous reactive sulfur species in the forefront in the electrophile detoxification pathway. *Sulfurtransferases,* 101-117.

Hamouda, S. A., Alshawish, N. K., Abdalla, Y. K., & Ibrahim, M. K. (2022). Ultraviolet radiation: Health risks and benefits. *Saudi Journal of Engineering and Technology,* 7(10), 533-541.

Hart, P. H., & Norval, M. (2021). The multiple roles of urocanic acid in health and disease. *Journal of Investigative Dermatology, 141(3),* 496-502.

Hart, P. H, & Norval, M. (2021). More than effects in skin: ultraviolet radiation-induced changes in immune cells in human blood. *Frontiers in immunology, 12,* 694086.

Hart, P. H, & Norval, M. (2018). Ultraviolet radiation-induced immunosuppression and its relevance for skin carcinogenesis. *Photochemical & photobiological sciences,* 77(12), 1872-1884.

Hart, P. H., Norval, M., Byrne, S. N., & Rhodes, L. E. (2019). Exposure to ultraviolet radiation in the modulation of human diseases. *Annual Review of Pathology: Mechanisms of Disease, 14(\),* 55-81.

Hayes, J. D., & Pulford, D. J. (1995). The glut athione S-transferase supergene family: regulation of GST and the contribution of the Isoenzymes to cancer chemoprotection and drug resistance part II. *Critical reviews in biochemistry and molecular biology, 30(6),* 521-600.

Hristov, B. D. (2022). The role of glutathione metabolism in chronic illness development and its potential use as a novel therapeutic target. *Cureus, 14(9).*

Holick, M. F. (2020). Sunlight, UV radiation, vitamin D, and skin cancer: how much sunlight do we need?. *Sunlight, Vitamin D and Skin Cancer,* 19-36.

Holecek, M. (2020). Histidine in health and disease: metabolism, physiological importance, and use as a supplement. *Nutrients,* 12(3), 848.

Hosseini, S. M. (2015). Role of oxidative and energy metabolism in skin aging and UV-B induced carcinogenesis (Doctoral dissertation, Universite de Bordeaux).

Hussein, R S., Bin Dayel, S., Abahussein, O., & El-Sherbiny, A. A. (2025). Influences on skin and intrinsic aging: biological, environmental, and therapeutic insights. *Journal of Cosmetic Dermatology, 24(2),* el6688.

Husain, N. (2022). Sulphide Donor Exhibits Cytoprotective and Antioxidative Activity in UV-induced HaCaT Cell Lines. *ASM Science Journal, 17,* 1-6.

Husain, N, Raub, R. A., Akbar, N. B. N. 'Adzan F., & Hamid, H. A. (2022). Reactive Sulphur Species and Exposome: A Perspective on Potential Role in Alleviating UV-Induced Stress. *Journal of Pharmaceutical Research International, 34,* 44-53. https://doi.org/10.9734/jpri/2022/v34i2b35379

Iciek, M., Bilska-Wilkosz, A., Kozdrowicki, M., & Gorny, M. (2022). Reactive sulfur species and their significance in health and disease. *Bioscience Reports, 42(9),* BSR20221006.

Jauhonen, H. M. (2017). *Effects of cis-urocanic addon ocular surface* (Doctoral dissertation, Ita-Suomen yliopisto).

Jimenez-Sanchez, M., Celiberto, L. S., Yang, H., Sham, H. P., & Vallance, B. A. (2025). The gut-skin axis: a bi-directional, microbiota-driven relationship with therapeutic potential. *GutMicrobes*, 77(1), 2473524.

Johal, K. S., Saour, S., & Mohanna, P. N. (2021). The skin and subcutaneous tissues. In *Browse's introduction to the symptoms & signs of surgical disease* (pp. 111-167). CRC Press.

Johns Hopkins Medicine, (n.d.). Anatomy of the skin. Retrieved January 1, 2026, from https://www.hopkinsmedicine.org/health/skin/anatomy-of-the-skin

Juzeniene, A., & Moan, J. (2012). Beneficial effects of UV radiation other than via vitamin D production. *Dermato-endocrinology, 4(2),* 109-117.

Kaneko, K., Smetana-Just, U., Matsui, M., Young, A. R., John, S., Norval, M., & Walker, S. L. (2008). c/5-Urocanic acid initiates gene transcription in primary human keratinocytes. *The Journal of Immunology, 181(1),* 217-224.

Kaneko, K., Walker, S. L., Lai-Cheong, J., Matsui, M. S., Norval, M., & Young, A. R (2011). c/5-Urocanic acid enhances prostaglandin E2 release and apoptotic cell death via reactive oxygen species in human keratinocytes. *Journal of investigative dermatology, 131(6),* 1262-1271.

Kasamatsu, S., & Ihara, H. (2021). Regulation of redox signaling by reactive sulfur species. *Journal of clinical biochemistry and nutrition, 68(2),* 111-115.

Kasamatsu, S., Kinno, A., Miura, C, Hishiyama, J. I., Fukui, K., Kure, S., ... & Ihara, H. (2024). Quantitative profiling of supersulfides naturally occurring in dietary meats and beans. *Analytical Biochemistry, 685,* 115392.

Kammeyer, A., Pavel, S., Asghar, S. S., Bos, J. D., & Teunissen, M. B. (1997). Prolonged increase of cz's-urocanic acid levels in human skin and urine after single total-body ultraviolet exposures. *Photochemistry andphotobiology, 65(3),* 593-598.

Kammeyer, A., Peters, C. P., Meijer, S. L., & Te Velde, A. A. (2012). Anti-inflammatory effects of urocanic Acid derivatives in models ex vivo and in vivo of inflammatory bowel disease. *International Scholarly Research Notices, 2012(1),* 898153.

Khodade, V. S., & Toscano, J. P. (2023). Reactive sulfur species in biology and medicine. *Antioxidants, 12(9),* 1759.

Kim, H. S., Kim, H. J., Hong, Y D., Son, E. D., & Cho, S. Y. (2023). P-endorphin suppresses ultraviolet B irradiation-induced epidermal barrier damage by regulating inflammation-dependent mTORC 1 signaling. *Scientific Reports, 13(1),* 22357.

Kinuta, M., Ohta, J., Yamada, H., Kinuta, K., Abe, T., Li, S. A., ... & Takei, K. (2001). Determination of S-[2-carboxy-l-(lH-imidazol-4-yl) ethyl] glutathione, a novel metabolite of 1-histidine, in tissue extracts from sunlight-irradiated rat by capillary electrophoresis. *Electrophoresis*, 22(16), 3365-3370.

Kinuta, M., Kinuta, K., Yamada, H., Abe, T., Yoshida, Y., Araki, K., ... & Takei, K. (2003). Formation of S-[2-carboxy-l-(lH-imidazol-4-yl) ethyl] glutathione, a new metabolite of L-histidine, from cis-urocanic acid and glutathione by the action of glutathione S-transferase. *Electrophoresis*, 2 ¥(18), 3212-3218.

Korhonen, E., Piippo, N., Hytti, M., Kaamiranta, K., & Kauppinen, A. (2023). Cz's-urocanic acid improves cell viability and suppresses inflammasome activation in human retinal pigment epithelial cells. *Biochemical Pharmacology, 216,* 115790.

Kolluru, G K., Shen, X., & Kevil, C. G (2020). Reactive sulfur species: a new redox player in cardiovascular pathophysiology. *Arteriosclerosis, thrombosis, and vascular biology, 40(4),* 874-884.

Kolluru, G. K., Shackelford, R. E., Shen, X., Dominic, P., & Kevil, C. G (2023). Sulfide regulation of cardiovascular function in health and disease. *Nature Reviews Cardiology, 20(2),* 109-125.

Kripke, M. L., Cox, P. A, Alas, L. G, & Yarosh, D. B. (1992). Pyrimidine dimers in DNA initiate systemic immunosuppression in UV-irradiated mice. *Proceedings of the National Academy of Sciences,* 59(16), 7516-7520.

Laihia, Jarmo K., Janne P. Kallio, Pekka Taimen, Harry Kujari, Veli-Matti Kahari, and Lasse Leino. "Protodynamic intracellular acidification by cz's-urocanic acid promotes apoptosis of melanoma cells in vitro and in vivo." *Journal of Investigative Dermatology* 130, no. 10 (2010): 2431-2439.

Laikova, K. V., Oberemok, V. V., Krasnodubets, A. M., Gal'chinsky, N. V., Useinov, R. Z., Novikov, I. A., ... & Kubyshkin, A. V. (2019). Advances in the understanding of skin cancer: ultraviolet radiation, mutations, and antisense oligonucleotides as anticancer drugs. *Molecules, 24(8),* 1516.

Lau, N., & Pluth, M. D. (2019). Reactive sulfur species (RSS): persulfides, poly sulfides, potential, and problems. *Current Opinion in Chemical Biology, 49,* 1-8.

Li, C, Cong, Y., & Deng, W. (2022). Identifying molecular functional groups of organic compounds by deep learning of NMR data. *Magnetic Resonance in Chemistry, 60(1*1), 1061-1069.

Li Pomi, F., Gammeri, L., Borgia, F., Di Gioacchino, M., & Gangemi, S. (2025). Oxidative Stress and Skin Diseases: The Role of Lipid Peroxidation. *Antioxidants*, *14(5)*, 555.

Licznerska, B., Szaefer, H., & Krajka-Kuzniak, V. (2021). R-sulforaphane modulates the expression profile of AhR, ERa, Nrf2, NQOl, and GSTP in human breast cell lines. *Molecular and Cellular Biochemistry, 476(2),* 525-533.

Lopez-Ojeda, W., Pandey, A., Alhajj, M., & Oakley, A. M. (2022). Anatomy, skin (integument). In *StatPearls [Internet]*. StatPearls Publishing.

Lu, B. W., Chao, G J., Wu, G. P., & Xie, L. K. (2021). In depth understanding of retinitis pigmentosa pathogenesis through optical coherence tomography angiography analysis: a narrative review. *International Journal of Ophthalmology, 14(12),* 1979.

Lu, H., Chen, Y., & Hu, P. (2023). Current Status and Future Prospects of Hydrogen Sulfide Donor-Based Delivery Systems. *Advanced Therapeutics, 6(5),* 2200349.

Lukic, M., Pantelic, I., & Savic, S. D. (2021). Towards optimal ph of the skin and topical formulations: From the current state of the art to tailored products. *Cosmetics, 8(3),* 69.

Mathews, L. A., Cabarcas, S. M., & Farrar, W. L. (2011). DNA repair: the culprit for tumor-initiating cell survival?. *Cancer and metastasis reviews, 30(2),* 185-197.

Mayo Clinic. (2025). *Basal cell carcinoma of the skin - Symptoms and causes.* Mayo Clinic.https://www.mayoclinic.org/diseases-conditions^asal-cell-carcinoma/symptoms-causes/syc-203 54187

Mayo Clinic. (2025). *Melanoma - Symptoms and causes.* Mayo Clinic.https://www.mayoclinic.org/diseases-conditions/melanoma/symptoms-causes/syc-20374884

McLoone, P., Simics, E., Barton, A., Norval, M., & Gibbs, N. K. (2005). An action spectrum for the production of czs-urocanic acid in human skin in vivo. *Journal of investigative dermatology, 124(5),* 1071-1074

Milner, S. M. (2023). Skin anatomy. *Eplasty, 23,* QA8.

Mirzayev, M. (2025). ANATOMY OF THE SKIN: STRUCTURE AND FUNCTIONS OF THE EPIDERMIS AND *DERMIS. International journal of medical sciences, 1(2),* 302-306.

Mo, C, Bajgai, J., Rahman, M. H., Choe, S., Abdul-Nasir, S., Ma, H., ... & Shin, I. (2025). A pilot clinical trial to explore the effects of UV exposure on vitamin D synthesis and inflammatory responses in vitamin D-Deficient adults. *Scientific Reports,* 75(1), 22557.

Mohania, D., Chandel, S., Kumar, P., Verma, V., Digvijay, K., Tripathi, D., ... & Shah, D. (2017). Ultraviolet radiations: Skin defense-damage mechanism. *Ultraviolet Light in Human Health, Diseases and Environment*, 71-87.

Mooney, M. K., Forsyth, C, Rae, I. J., Chisham, G, Coxon, J. C, Marsh, M. S., ... & Hubert, B. (2020). Examining local time variations in the gains and losses of open magnetic flux during substorms. *Journal of Geophysical Research: Space Physics*, 725(4), e2019JA027369.

Moosbrugger-Martinz, V., Leprince, C, Mechin, M. C, Simon, M., Blunder, S., Gruber, R., & Dubrac, S. (2022). Revisiting the roles of filaggrin in atopic dermatitis. *International Journal of Molecular Sciences,* 23(10), 5318.

Munteanu, C, Turnea, M. A., & Rotariu, M. (2023). Hydrogen Sulfide: An emerging regulator of oxidative stress and cellular homeostasis—a comprehensive one-year review. *Antioxidants, 12(9), 1131*.

Nagana Gowda, G. A., Pascua, V., Neto, F. C, & Raftery, D. (2022). Hydrogen-Deuterium Addition and Exchange in N-Ethylmaleimide Reaction with Glutathione Detected by NMR Spectroscopy. *ACS omega,* 7(30), 26928-26935.

Norval, M., Gibbs, N. K., & Gilmour, J. (1995). The role of urocanic acid in UV-induced immunosuppression: recent advances (1992-1994). *Photochemistry and photobiology, 62(2),* 209-217.

Norval, M., McLoone, P., Lesiak, A., & Narbutt, J. (2008). The effect of chronic ultraviolet radiation on the human immune system. *Photochemistry and Photobiology, 84(1),* 19-28.

Norval, M. (2001). Effects of solar radiation on the human immune system. *Comprehensive Series in Photosciences, 3,* 91-113.

Norval, M., & El-Ghorr, A. A. (2002). Studies to determine the immunomodulating effects of cis-urocanic acid. *Methods,* 25(1), 63-70.

Norval, M., & El-Ghorr, A. A. (2002). Studies to determine the immunomodulating effects of cis-urocanic acid. MetNorval, M., & Woods, G M. (2011). UV-induced immunosuppression and the efficacy of vaccination. Photochemical & Photobiological Sciences, 10(8), 1267-1274.hods, 28(1), 63-70.

Norval, M., & Halliday, G M. (2011). The consequences of UV-induced immunosuppression for human health. *Photochemistry and photobiology, 87(5),* 965-977.

Oakley, A. (2011). Glutathione transferases: a structural perspective. *Drug metabolism reviews, 43(2),* 138-151.

Oakley, A. J., Bello, M. L., Nuccetelli, M., Mazzetti, A. P., & Parker, M. W. (1999). The ligandin (non-substrate) binding site of human Pi class glutathione transferase is located in the electrophile binding site (H-site). *Journal of molecular biology, 291(4),* 913-926.

Panich, U., Sittithumcharee, G., Rathviboon, N., & Jirawatnotai, S. (2016). Ultraviolet radiation-induced skin aging: the role of DNA damage and oxidative stress in epidermal stem cell damage-mediated skin aging. Stem cells international, 2016(1), 7370642.

Pandey, T., & Pandey, V. (2024). Advancements in increasing efficiency of hydrogen sulfide in therapeutics: Strategies for targeted delivery as prodrugs. *Nitric Oxide, 152,* 1-10.

Peate, I. (2021). The skin: largest organ of the body. *British Journal of Healthcare Assistants, 15(9),* 446-451.

Peuhu, E., Kaunisto, A., Laihia, J. K., Leino, L., & Eriksson, J. E. (2010). Molecular targets for the protodynamic action of cz's-urocanic acid in human bladder carcinoma cells. *BMC cancer,* 70(1), 521.

Peltonen, J. M., PyLKKaNEN, L., JANSeN, C. T., Volanen, I., Lehtinen, T., Laihia, J. K., & Leino, L. (2014). Three randomised phase I/IIa trials of 5% cz's-urocanic acid emulsion cream in healthy adult subjects and in patients with atopic dermatitis. *Acta Dermato-Venereologica, 94(4),* 415-420.

Pellerin, L., Henry, J., Hsu, C. Y., Balica, S., Jean-Decoster, C, Mechin, M. C, ... & Simon, M. (2013). Defects of filaggrin-like proteins in both lesional and nonlesional atopic skin. *Journal of allergy and clinical immunology, 131(4),* 1094-1102.

Pham, D. L., Lim, K. M., Joo, K. M., Park, H. S., Leung, D. Y., & Ye, Y. M. (2017). Increased *cis-to-trans* urocanic acid ratio in the skin of chronic spontaneous urticaria patients. *Scientific Reports,* 7(1), 1318.

Prakash, M., Shetty, M. S., Tilak, P., & Anwar, N. (2009). Total thiols: biomedical importance and their alteration in various disorders. *Online J Health Allied Scs, 8(2), 2.*

Prasetyawan, F., Saristiana, Y., Megasari, E., & Indrayanti, D. (2025). Halal Studies & Prediction of Sulforaphane From Cabbage (Brasica Oleracia var. capitata L.) As Glutathione S-Transferase (GST) Substrate. *Iqro Bhisma (IB): Jurnal Studi Ilmu Keagamaan Islam,* 7(1), *64-11*.

Prohic, A. (2024). Skin Structure and Functions of the Skin. *In Dermatovenerology Textbook* (pp. 3-15). Cham: Springer Nature Switzerland.

Reeve, V. E., Greenoak, G E., Canfield. P. J., Boehm-Wilcox, C. H. R. I. S. T. A, & Gallagher, C. H. (1989). Topical urocanic acid enhances UV-induced tumour yield and malignancy in the hairless mouse. *Photochemistry andPhotobiology, 49(4),* 459-464.

Reich, A., & M^drek, K. (2013). Effects of narrow band UVB (311 nm) irradiation on epidermal cells. *International journal of molecular sciences, 14(4),* 8456-8466.

Rieko, K. K., & Motonobu, N. (2016). Effect of cz's-urocanic acid on atopic dermatitis in NC/Ngamice. *Journal of Dermatological Science, 84(1),* e65-e66.

Sadhu, S. S., Wang, S., Dachineni, R, Averineni, R. K., Seefeldt, T., Xie, J., ... & Guan, X. (2017). In vitro and in vivo antimetastatic effect of glutathione disulfide liposomes. *Cancer growth and metastasis, 10,* 1179064417695255.

Salah, A. & Ragab, M. (2025). *Molecular Spectroscopy in Organic Chemistry: IR, NMR, and Mass Analysis.*

Salminen, A., Kaarniranta, K., & Kauppinen, A. (2022). Photoaging: UV radiation-induced inflammation and immunosuppression accelerate the aging process in the skin. *Inflammation Research, 71(7),* 817-831.

Schrodinger, L. L. C. (2015). ThePyMOL molecular graphics system. *Version, 1,* 8.

Sciskalska, M., & Milnerowicz, H. (2020). The role of GSTTC isoform in the cells signalling and anticancer therapy. *European Review for Medical & Pharmacological Sciences, 24(16).*

Shakeel, S., Tariq, M., Arif, N., Malik, A., Abid, M., Kausar, S., & Shahzadi, S. (2025). The role of uv radiation in chromosomal mutations: mechanisms, impacts, and implications for genomic stability. *Global Research Journal of Natural Science and Technology, 3(1).*

Shehu, D., Abdullahi, N., & Alias, Z. (2019). Cytosolic glutathione S-transferase in bacteria: a review. *Polish Journal of Environmental Studies, 28(2).*

Solano, F. (2020). Metabolism and functions of amino acids in the skin. *Amino Acids in Nutrition and Health: Amino acids in systems function and health,* 187-199.

Song, S., Li, F., Zhao, B., Zhou, M., & Wang, X. (2025). Ultraviolet light causes skin cell senescence: from mechanism to prevention principle. *Advanced Biology, 9(2),* 2400090.

Tan, S. P., Brown, S. B., Griffiths, C. E., Weller, R. B., & Gibbs, N. K. (2017). Feeding filaggrin: effects of 1-histidine supplementation in atopic dermatitis. *Clinical, Cosmetic and Investigational Dermatology,* 403-411.

Tew, K. D. (2007). Redox in redux: Emergent roles for glutathione S-transferase P (GSTP) in regulation of cell signaling and S-glutathionylation. *Biochemical pharmacology, 73(9),* 1257-1269.

Tirka, P. S. W., Praharsini, I. G. A. A., Karmila IGAAD, R. L., Suryawati, N., & Vibriyantikarna, N. L. P. R (2023). High serum level of matrix metalloproteinase-1 (MMP-1) correlates positively with The severity of photoaging facial wrinkles. *IntJSci Adv [Internet], 4(1).*

Toyokuni, S., Hirao, A., Wada, T., Nagai, R., Date, A., Yoshii, T., ... & Kawada, A. (2011). Age-and sun exposure-dependent differences in 8-hydroxy-2'-deoxyguanosine and Ns-(carboxymethyl) lysine in human epidermis. *Journal of Clinical Biochemistry and Nutrition, 49(2),* 121-124.

Tuna, D., Sporkel, L., Barbatti, M., & Thiel, W. (2018). Nonadiabatic dynamics simulations of photoexcited urocanic acid. *Chemical Physics, 515,* 521-534.

Valdes-Tresanco, M. S., Valdes-Tresanco, M. E., Valiente, P. A., & Moreno, E. (2020). AMDock: a versatile graphical tool for assisting molecular docking with Autodock Vina and Autodock4. *Biology direct, 15(1),* 12.

Verma, A., Zanoletti, A., Kareem, K. Y., Adelodun, B., Kumar, P., Ajibade, F. O., ... & Dwivedi, A. (2024). Skin protection from solar ultraviolet radiation using natural compounds: a review. *Environmental Chemistry Letters, 22(1),* 273-295.

Vieyra-Garcia, P. A., & Wolf, P. (2021). A deep dive into UV-based phototherapy: Mechanisms of action and emerging molecular targets in inflammation and cancer. *Pharmacology & therapeutics, 222,* 107784.

Vollmer, M. (2021). Physics of the electromagnetic spectrum. *Electromagnetic technologies in food science,* 1-32.

Walterscheid, J. P., Nghiem, D. X., Kazimi, N, Nutt, L. K., McConkey, D. J., Norval, M., & Ullrich, S. E. (2006). Cz's-urocanic acid, a sunlight-induced immunosuppressive factor, activates immune suppression via the 5-HT2A receptor. *Proceedings of the National Academy of Sciences, 103(46),* 17420-17425.

Walterscheid, J. P., Ullrich, S. E., & Nghiem, D. X. (2002). Platelet-activating factor, a molecular sensor for cellular damage, activates systemic immune suppression. *The Journal of experimental medicine, 195(2),* 171-179.

Wei, G (2019). Role of urocanic acid as an endogenous photoprotectant and as a therapeutic target for treating UV-induced melanoma and non-melanoma malignancies (Doctoral dissertation).

Welch, D., Aquino de Muro, M., Buonanno, M., & Brenner, D. J. (2022). Wavelength-dependent DNA photodamage in a 3-D human skin model over the far-UVC and

germicidal UVC wavelength ranges from 215 to 255 nm. *Photochemistry and Photobiology*, *98*(5), 1167-1171.

Yadav, T. C., Srivastava, A. K., Dey, A., Kumar, N., Raghuwanshi, N., & Pruthi, V. (2018). Application of computational techniques to unravel structure-function relationship and their role in therapeutic development. *Current Topics in Medicinal Chemistry*, *18*(20), 1769-1791.

Ye, Y. M., Kim, B. E., Shin, Y. S., Park, H. S., & Leung, D. Y. (2014). Increased epidermal filaggrin in chronic idiopathic urticaria is associated with severity of urticaria. *Annals of Allergy, Asthma & Immunology*, *112*(6), 533-538.

Yoo, S., Kim, J., Jeong, E. T., Hwang, S. J., Kang, N. G., & Lee, J. (2024). Penetration rates into the stratum corneum layer: A novel quantitative indicator for assessing skin barrier function. *Skin Research and Technology*, *30*(3), e13655.

Yu, X. D., Li, A., Li, X. Y., Zhou, Y., Li, X., He, Z., ... & Shu, X. (2022). *Trans*-urocanic acid facilitates spatial memory, implications for Alzheimer's disease. *Physiology & Behavior*, *252*, 113827.

Yu, C. (2016). Modulation of immune responses by UV irradiation.

Zhang, T., Akaike, T., & Sawa, T. (2024). Redox regulation of xenobiotics by reactive sulfur and supersulfide species. *Antioxidants & Redox Signaling*, *40*(10-12), 679-690.

Zhu, H., Wang, N., Yao, L., Chen, Q., Zhang, R., Qian, J., ... & Xiong, W. (2018). Moderate UV exposure enhances learning and memory by promoting a novel glutamate biosynthetic pathway in the brain. *Cell*, *173*(7), 1716-1727.

Zorina, A., Zorin, V., Kudlay, D., & Kopnin, P. (2022). Molecular mechanisms of changes in homeostasis of the dermal extracellular matrix: both involutional and mediated by ultraviolet radiation. *International Journal of Molecular Sciences*, *23*(12), 6655.

Zuberbier, T., Abdul Latiff, A. H., Abuzakouk, M., Aquilina, S., Asero, R., Baker, D., ... & Maurer, M. (2022). The international EAACI/GA²LEN/EuroGuiDerm/APAAACI guideline for the definition, classification, diagnosis, and management of urticaria. *Allergy*, *77*(3), 734-766.

AUTHOR'S PROFILE

Aina Yusrina binti Ali Musa obtained her degree in Bachelor of Biotechnology (Hons) program at Universiti Selangor (UniSel), where she graduated with First-Class Honours in 2022. In 2023, she began her Master of Science in Pharmacology at Universiti Teknologi MARA. Her master's research, titled "Metabolic Pathway of Uraconic Acid (UCA) upon Ultraviolet B (UVB) Exposure using ^{1}H Nuclear Magnetic Resonance (NMR) Spectroscopy, Molecular Docking and Cell Viability of Human Keratinocytes (HaCaT) Cell Lines", focuses on skin health and combines *in silico* molecular docking with *in vitro* experimental approaches. She has published an article titled "Yin and yang of urocanic acid in skin pathogenesis: A mini review on its metabolism and effects" and is preparing additional manuscripts based on her research findings.

LIST OF PUBLICATION:

Ali Musa, A. Y., Abdul Hamid, H, & Husain, N. (2025). Ying and yang of urocanic acid in skin pathogenesis: a mini review on its metabolism and effects. *International Journal of Pharmaceutical, Nutraceutical and Cosmetic Science (IJPNaCS),* 5(1), 71-81.

PERPUSTAKAAN TUN ABDUL RAZAK
BAHAGIAN SUMBER RUJUKAN UNIVERSITI (BSRU)

BORANG PENYERAHAN BAHAN HARTA INTELEK UiTM

UiTM's Intellectual Property Submission Form

Nama (*Name*) **:** AINA YUSRINA BINTI ALI MUSA

Fakulti/Pusat Akademik/Bahagian : FAKULTI FARMASI
Faculty / Academic Centres / Department

No. Telefon (Pejabat / Hp) : 0172100428
Telephone No. (Office / handphone)

E-mel (E-mail) **:** aiysri00@gmail.com

Tarikh (*Date*) **:** 10 APRIL 2026

Pihak Fakulti / Pusat Akademik / Bahagian / Saya bersetuju bahawa dokumen dan tajuk yang disenaraikan untuk dimasukkan ke dalam Repositori Institusi UiTM.
The Faculty / Academic Centres / Department / I agree that the document and titles listed below to be placed in the UiTM Institutional Repository.

JENIS BAHAN (Sila nyatakan) : THESES
Types of Material (Please specify) :

Types of Material:
Article / Book / Theses / Bulletin / Seminar / Image / Entrepreneurship / Student Project / Research Report / Industrial Training / Annual Report / Manual / Oral History / Exam Paper / Speech / Dataset / Audio / Video / Others

MAKLUMAT BAHAN *(Information of Materials)*:

Bil. *No.*	**JUDUL BAHAN** *Title*	**HARDCOPY** *(√)*	**SOFTCOPY** *(√)*
1.	*RUJUK KEPADA LAMPIRAN		/

**** Sila sediakan lampiran sekiranya ruangan yang disediakan tidak mencukupi*** *(Please provide attachment if necessary)*

TUJUAN PENYERAHAN BAHAN (Sila tandakan √):

Purpose (Please mark √):

1. **Bahan untuk dimuat naik ke dalam Repositori Institusi UiTM:** [/]
   (Materials for uploading into the UiTM Institutional Repository (UiTM IR)):
   Fakulti / Pusat Akademik / Bahagian / Saya perlu memastikan bahawa setiap dokumen telah dibuat semakan terlebih dahulu dan tidak mengandungi sebarang maklumat sulit sebelum diserahkan kepada pihak PTAR.
   The Faculty / Academic Centres / Department must ensure that each document has been reviewed in advance and does not contain any confidential information before being submitted to PTAR).
2. **Bahan mengandungi maklumat TERHAD yang telah ditentukan oleh organisasi / badan di mana penyelidikan dijalankan:** [ ]
   (Materials consisting of RESTRICTED information which has been determined by the organisation/body where the research was conducted):
   Sila nyatakan tarikh tamat embargo (jika ada)*:*
   (Please indicate the embargo expiry date (if any)):
   Embargo expiry date: Day: [ ] *Month:* [ ] *Year:* [ ]

   Nota: Embargo Expiry Date adalah tarikh tamat tempoh yang ditetapkan oleh penulis di mana pada atau selepas tarikh ini, bahan tersebut akan dipaparkan secara langsung di Repositori Institusi UiTM dan ianya boleh diakses.
   Note: Embargo Expiry Date *is the date that an author or a publisher imposed embargo expires. On and after this date, this document will be accessible in UiTM Institutional Repository.*
3. **Bahan boleh diakses secara teks penuh dan terbuka.** [/]
   (Materials can be accessed in full text via open access).
4. **Bahan dipinjamkan sementara untuk tujuan pendigitalan dan akan dikembalikan semula kepada pemilik.** [/]
   (Materials are on temporary loan for digitization and will be returned to the owner).

Pemberitahuan: Jika Repositori Institusi UiTM menerima bukti pelanggaran hak cipta, bahan yang berkaitan akan dikeluarkan serta-merta.
(Notification: If UiTM Institutional Repository receives proof of copyright violation, the relevant item will be removed immediately).

PERAKUAN:

Declaration:

Saya / kami akan bertanggungjawab ke atas bahan yang diserahkan untuk pendigitalan dan muat naik ke dalam Repositori Institusi UiTM.
I / we will be responsible for the materials submitted for digitization and uploaded into UiTM Institutional Repository.

_____
Tandatangan Pemohon
Applicant Signature
Tarikh (*Date*):

_____
Tandatangan dan Cap Ketua Jabatan / Bahagian / Penyelia
Head of Division / Department / Supervisor Signature and stamp
Tarikh (*Date*):

UNTUK KEGUNAAN PEJABAT (*For office use*)

DITERIMA OLEH / *Received By* :
TANDATANGAN / *Signature* :
TARIKH / *Date* :

DISAHKAN OLEH / Certified *By* :
TANDATANGAN / *Signature* :
TARIKH / *Date* :